International Journal of Microwave and Wireless Technologies

cambridge.org/mrf

A review on circularly polarized antennas, trends and advances

Utsab Banerjee[1], Anirban Karmakar[1] and Anuradha Saha[2]

[1]Electronics & Communication Engineering Department, Tripura University (A Central University), Tripura, India and [2]Department of A.E.I.E., Netaji Subhash Engineering College, Garia, Kolkata, India

Tutorial and Review Paper

Cite this article: Banerjee U, Karmakar A, Saha A (2020). A review on circularly polarized antennas, trends and advances. *International Journal of Microwave and Wireless Technologies* **12**, 922–943. https://doi.org/10.1017/S1759078720000331

Received: 11 September 2019
Revised: 18 March 2020
Accepted: 19 March 2020
First published online: 16 April 2020

Key words:
Antennas; axial ratio; bandwidth; circular polarization; left hand circular polarization; right hand circular polarization

Author for correspondence:
Utsab Banerjee, E-mail: utsabbanerjee36@gmail.com

Abstract

This literature presents a comprehensive, technical review of circularly polarized (CP) antennas for different applications in wireless communication, emphasizing on the recent developments in the concerned research. The article also presents a comparative study of various works reported in the open literature, with an aim to highlight the contribution of CP antenna systems in the chronological development of the wireless communication technology. The primary motive of this review is to (a) highlight the methodologies used by different researchers to portray and analyze the different aspects in which CP antennas find their applications in modern-day wireless communication, (b) provide a practical viewpoint of the future scope of the study, based upon the past and present state-of-art research trends and (c) provide a conceptual and technical support to present-day antenna designers to help the process of furtherance of innovation and multiple system integration. In conclusion, the article also throws some light upon the future scope of research in the vast domain of CP antenna applications.

Introduction

Polarization is one of the most essential and significant features of an antenna in modern wireless communication systems [1]. Polarization of an antenna is the locus traced out by the tip of the electric field vector of the wave radiated or received by the antenna as a function of time. Polarization of an antenna is usually determined from the electric field orientation; it will be either linearly or circularly polarized (CP) [1]. The orientation of the electromagnetic field radiated by a linearly polarized antenna lying in one plane, orthogonal to the direction of electromagnetic wave propagation. For example, a vertically polarized antenna can efficiently transmit and receive only a vertically polarized wave and vice versa, which is known as co – polarization [2]. Due to the reciprocity property of the antenna, the transmission and reception of the antenna are always similar. If a receiving antenna is vertically polarized and a transmitting antenna is horizontally polarized, then it is called cross-polarization [2], which incurs a huge signal loss. In circular polarization the antenna emits electromagnetic energy in a circular spiral pattern which covers horizontal, vertical, and all the planes in-between them. With circular polarization, the orientation of the transmitting and receiving antennas is irrelevant as the circular pattern of the transmitting and/or receiving antenna will always match with pattern of the incoming signal. Among other salient advantages of CP antennas are multipath rejection, which leads to signal interference in linear polarization, mitigation of fading effects and immunity against Faraday rotation effect, which make CP antennas somewhat indispensable components in modern wireless communication systems [2].

In the case of circular polarization, the orthogonal field components are almost of equal amplitude, spatially orthogonal and in phase quadrature. Thus the tip of the resultant electric field vector generates a circular locus while evolving in time.

In linear polarization, Fig. 1(a), the tip of the electric field vector oscillates along the same line, here along the x- or y-axes, thus tracing out a straight line.

In the case of elliptical polarization, shown in Fig. 1(c), however, the quadrature-phase difference between the two field components is maintained, but the field components may not be of the same magnitude, as in circular polarization, shown in Fig. 1(b). So, circular polarization may be considered as a special case of elliptical polarization. Circular polarization is quantified by the axial ratio (AR) [1], which is the ratio of the maximum and minimum semi-axes of the polarization ellipse and is given in decibels by:

$$AR(dB) = 20\log_{10}\left[\frac{E_{x_0}}{E_{y_0}}\right], \tag{1}$$

from which it can be noticed that $1 \leq AR < \infty$. A pure circular polarization can be achieved when $AR = 1$ or 0 dB, which is difficult to achieve in practice. Therefore, a frequency range

© Cambridge University Press and the European Microwave Association 2020

CAMBRIDGE UNIVERSITY PRESS

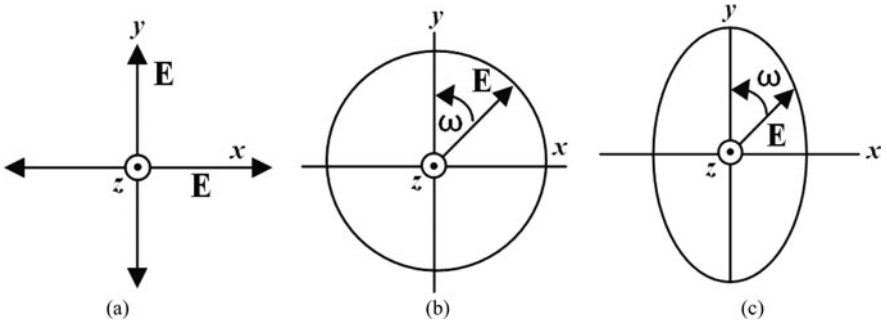


Fig. 1. Electric field vector tracing (a) linear, (b) circular, and (c) elliptical polarizations [1].

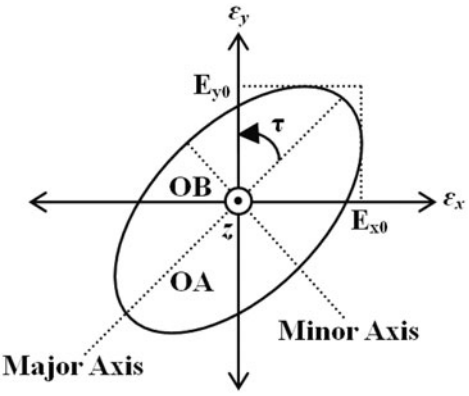


Fig. 2. Polarization ellipse showing parameters of polarization [1].

over which $AR \leq 3$ dB is considered, and defined as

$$Axial\ Ratio\ Bandwidth = \frac{f_2 - f_1}{f_{min}}, \tag{2}$$

where, f_1 and f_2 are the boundary frequencies for $AR \leq 3$ dB and f_{min} is the frequency of minimum value of AR. The polarization ellipse is shown in Fig. 2, where the major and the minor axes are shown. E_{x_0} and E_{y_0}, mentioned in (1) are the maximum values of the electric field magnitude on these axes. For circular polarization, these values are equal. So, circular polarization is a special case of elliptical polarization. Also, it is seen from Fig. 2 that the orientation of the ellipse is defined by another parameter, the tilt angle (τ), which is the inclination of the major axis of the ellipse with respect to the vertical axis. OA and OB represent the major and minor axes of the polarization ellipse, respectively, while E_{x_0} and E_{y_0} represent the maximum magnitudes of the electric field along the x- and y-directions.

A general planar microstrip patch antenna on its own does not radiate CP wave; subsequently, some modifications should be done to the patch antenna to be able to generate the circular polarization [3–10]. In the following sections of this review, a detailed discussion is presented about the various techniques adopted by researchers to generate circular polarization. Each categorical description includes the basic methodologies, progressive evolution of design trends, and comparative study of different antennas reported in the literature. CP microstrip antennas can be classified according to the number of feeding points required to produce CP waves. The most widely used feeding networks incorporated are dual or multiple feed and single feed.

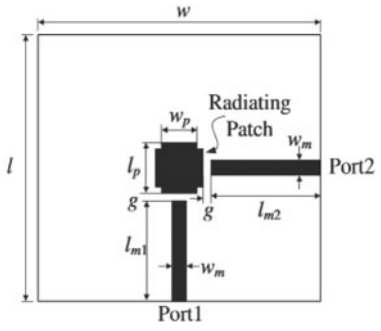


Fig. 3. Example of dual-fed CP patch [4].

Dual feeding network

As 90° phase shift between the orthogonal fields in the microstrip antenna is a mandatory pre-requisite for having circular polarization, dual feed is an obvious way to generate circular polarization in microstrip antenna. The two feed points are chosen spatially orthogonal [4] to each other as shown in Fig. 3. With the help of an external polarizer, the microstrip patch antenna is fed by signals which are equal in magnitude and in phase quadrature. The substrate has the dimensions of $w = 45$ mm, $l = 55$ mm, the feed lines have width $w_m = 3.5$ mm, and lengths $l_{m1} = 18$ mm, $l_{m2} = 16.5$ mm. The gap g is taken to be 1 mm in dimension. Dual feed operation can be carried out using quadrature hybrid coupler, ring hybrid coupler, Wilkinson power divider, T-junction power splitter or two coaxial feeds with a physical phase shift of 90° [3, 6]. Generally, dual-fed CP antennas have a comparatively wider operational bandwidth. But this comes at the cost of increased design complexity to achieve satisfactory CP performance.

Single feeding structures

Single fed microstrip antennas are structurally simple, easy to fabricate, low cost and compact in structure as shown in Fig. 4. It eliminates the use of a complex hybrid polarizer, which is very complicated to be put in physical use [7]. Single fed CP microstrip antennas are considered to be one of the simplest antennas that can produce circular polarization [8]. In order to achieve CP using only a single feed, two degenerate modes should be exited with equal amplitude and 90° phase difference. Since basic shapes microstrip antenna produces linear polarization there must be some changes in the design to produce circular polarization. Perturbation segments are used to split the field into two orthogonal modes with equal magnitude and 90° phase shift. Therefore

https://doi.org/10.1017/S1759078720000331 Published online by Cambridge University Press

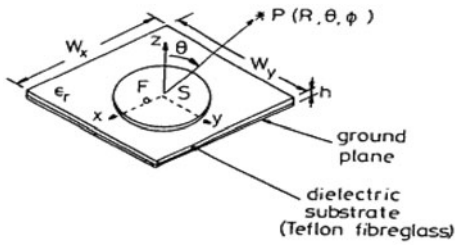


Fig. 4. Example of single-fed CP patch Antenna [7].

the circular polarization requirements are met. The most prominent advantage of single fed CP antennas is simplicity in design. But on the contrary, single fed CP antennas have a narrow operational bandwidth and so there has to be some additional mechanism to increase the operational bandwidth while maintaining the structural simplicity. Acceptability of the design depends upon these mechanisms and optimized results.

In general, CP antennas can be created in a wide number of ways. A method to generate CP waves is by introducing perturbation [3, 9, 10] in the antenna. The small perturbation has to be coherent with the desired frequency to produce two orthogonally polarized components with the same amplitude and a 90° phase difference.

Single feeding techniques are mostly adopted in modern microstrip antenna designs as they are simple, easy to fabricate, low in cost and compact in structure.

Several techniques [7–14] were used to achieve circular polarization in single fed microstrip antenna. Some of these are discussed here. In [7], a single-fed CP patch antenna has been shown which is fabricated on a Teflon fiberglass substrate of height "h" = 1.2 mm, "W_x" = 27 mm, "W_y" = 27 mm. The radius of the circular disc radiator is 10.5 mm. Till date, some review analysis has been performed on individual aspects of CP antennas, like circularly polarized dielectric resonator antennas [15, 16], fractal CP Antennas etc. But a comprehensive review of CP antennas as a whole, along with the vast domain of their applications is rare in the existing literature. This review article is an effort to fill up that void in the research document.

However, CP antennas can be classified into different types, based upon various aspects. This can be seen in the following set of flowcharts (Fig. 5).

CP wide band antennas

Generally, as pre-mentioned, there are two major techniques to generate circular polarization, single feed [7–10] and dual or multiple feed [2, 3, 6]. Most of the single feed CP antennas, although structurally simple; suffer from significantly narrow CP (3-dB) *AR* bandwidth and impedance bandwidths [7–9,14]. The huge requirement of modern-day high data rate communication among interacting systems inherits the necessity of increased bandwidth to accommodate this bulk data transmission. Correspondingly, the single-fed antennas cannot be used in wide band applications [17,18]. However, the dual-feed CP antennas generate a wider AR bandwidth but come along with additional design complexity. The printed CP slot antenna is suitable to use for improving operating bandwidth without increasing the substrate thickness or antenna size. The slot antenna with wide-slot aperture can provide greater bandwidth and have better manufacturing tolerances as compared to a conventional microstrip patch antenna [19]. Several types of techniques are proposed to improve AR bandwidth of the CP antennas. One of them is the creation of antenna array configuration with wideband hybrid couplers and power dividers. This technique could considerably increase AR bandwidth up to 20% [20] or by using four-element antennas over to 163% [21] but these approaches may not be feasible in specific applications with constrained dimensional flexibility. Also, these approaches make the feeding network exceedingly complex for practical fabrication. However, an obvious choice yielding wide impedance and CP bandwidth with planar and compact structure is the slot antenna [22–24]. The most attractive feeding method of wideband CP slot antennas is microstrip line and coplanar waveguide (CPW). Several types of various-shaped wide-slot antennas for improving CP radiation have been reported. These include asymmetric aperture antenna using CPW feed with 68% [19], L-shaped slot antenna providing 46.5% AR bandwidth [22], microstrip-fed circular slot antenna [23], and a CPW-fed square slot antenna with AR bandwidth 49% [24].

In [24], a CPW-fed broadband CP antenna is shown, which is fabricated on FR4 substrate of dimensions $60 \times 60 \times 0.8$ mm^3.The square slot side length is $L = 40$ mm. Within the slot there is a lightning-shaped feed-line of length $s = 36$ mm, which is connected to a vertical feed line, as shown in Fig. 6(a), having dimensions of $w_f = 4.2$ mm, $w_s = 2.5$ mm, $l_n = 10$ mm. On two opposite corners of the slot, there are two L-shaped strips defined by the dimension $d = 15$ mm. The lightening-shaped feed line protruded from the CPW and the pair of inverted-L grounded strips both contribute to the generation of CP radiation. The vertical and horizontal tuning stubs have effectively widened the return loss bandwidth, as seen in Figs 6(b) and 6(c). The measured antenna gain in the broadside direction considered within the 3-dB AR band of 2075–3415 MHz are reported to be within 2.6–4.2 dBic, which are large enough for short-range wireless communication systems.

32.2% AR bandwidth and 132% impedance bandwidth with more complex geometries have been presented in [25]. A wideband microstrip line-feed CP slot antenna was proposed using the dual-feed with an integrated ultra wideband (UWB) phase shifter in multi-layer structure [26]. CP bandwidth of the antenna is 54%. Recently, another microstrip-fed CP wide slot antenna with 90.2% and impedance and 40% AR bandwidths has been presented in [27].

For high-speed data transmission and/or multifunctional services, broadband CP antennas are often demanded. In recent years, a number of broadband CP antennas have been proposed [28–42]. Broadband circular polarization may be achieved by traveling-wave antennas [28–31], crossed dipoles [32–34], stacked patches [35–38], or broadband 90° hybrid feed networks [39–42]. Traveling-wave antennas usually need a broadband balun [29] or a transformer [30] for impedance matching. The traveling-wave aperture antenna proposed in [31] needs a cavity and the 3-dB AR bandwidth, which is about 21% for the antenna element. The crossed triangular bowtie dipole antenna developed in [32] also needs a feeding balun. The 3-dB AR bandwidths achieved by crossed-dipole antennas through a 90° phase delay line are 28.6% in [33] and 27% in [34], respectively. The H-shaped stacked patch achieves an AR bandwidth of 19.4% [35] while the aperture-fed patch antenna has an AR bandwidth of 33.6% [36]. The cavity-backed aperture stacked patch antenna provides an AR bandwidth of 43.3% [37] while the single-fed stacked patch antenna in [38] features an AR bandwidth of about

https://doi.org/10.1017/S1759078720000331 Published online by Cambridge University Press

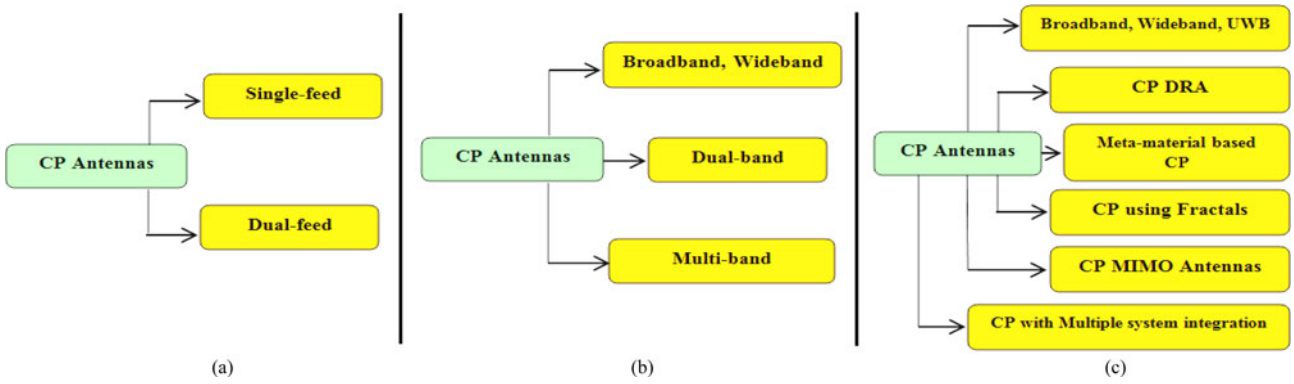


Fig. 5. Flowcharts showing different classifications of CP antennas based on (a) number of feeds, (b) bandwidth achieved, and (c) antenna structure.

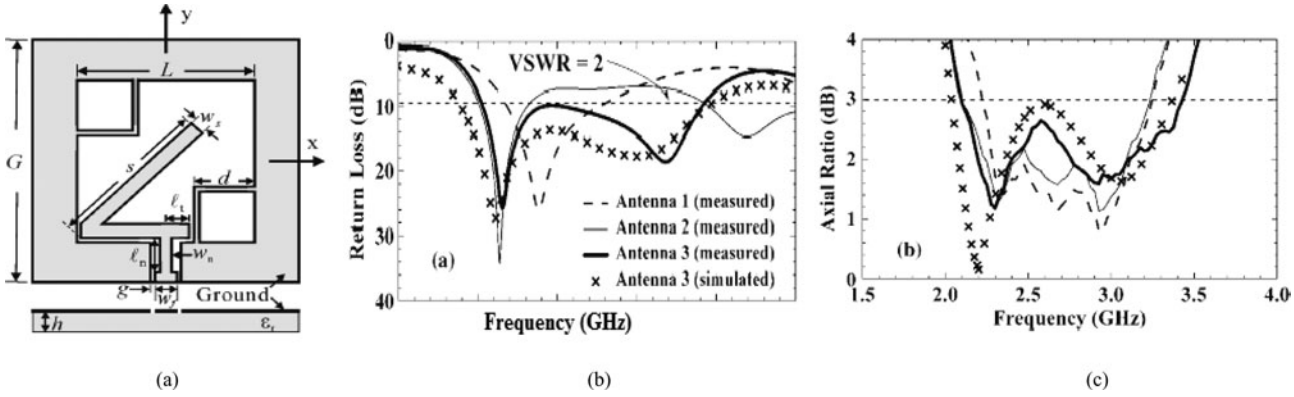


Fig. 6. A CPW-fed broadband CP antenna showing (a) proposed structure, (b) return loss bandwidth, (c) axial ratio bandwidth [24].

20.7%. The CP antennas using a broadband 90° hybrid feed network usually exhibit a broad AR bandwidth, e.g., 38% in [39], 33% in [40], 51.8% in [41], and 16% in [42]. Stacked patches and/or 90° hybrid feed networks may complicate the antenna design and fabrication.

In recent years, there has been growing interest in UWB antenna technology for short-range, high data rate wireless communication. Hence, research in the design of UWB equipments and antennas has received progressive attention. These antennas usually attempt to match the Federal Communications Commission (FCC) specified bandwidth covering from 3.1 to 10.6 GHz in its report in 2002 [43, 44], which is known as the UWB spectrum. In most cases, the monopole UWB antenna is widely used due to their lightweight, wide impedance bandwidth, good radiation characteristic, easy of fabrication and low cost. However, most of the UWB monopole antennas designs are based on linear polarization [45–48]. Indeed, the UWB technology is limited by distance due to very low transmitting power. To obtain distance gain, and also other pre-mentioned benefits the use of circular polarization (CP) in UWB technology is advantageous. The UWB CP antennas are used widely in military applications such as electronic countermeasure system, UWB radar, and medical applications [49].To obtain UWB CP, some design techniques have been studied [49–51]. In [49], the authors use an inverted–L shape in the ground plane to generate a resonant mode for broadband impedance bandwidth and excite two orthogonal electric field vectors with equal amplitude and 90° phase differences. In addition, cutting a bevel in the radiator patch increases the impedance bandwidth. This article consists of another design which is an I-shaped stub in the ground plane and a slot in rectangular radiator patch. In the second design, the impedance bandwidth increased compared to the first design frequency, from 2.17 to 8.47 GHz, hence, could not cover the whole of UWB frequency. In [50], a CPW-fed monopole antenna with wideband circular polarization is reported. The monopole, an upper parasitic strip and a modified parasitic Hilbert strip are coupled together by proximity coupling yielding a significantly wide impedance bandwidth. The antenna has an impedance bandwidth ranging from 2.04 to 7.95 GHz (118.2%) and an AR bandwidth ranging from 3.6 to 6.84 GHz (62%), thus covering the WLAN 5.2/5.8 GHz, the WiMAX 3.5/5.5 GHz and also partially covering the C-band (4–8 GHz). The antenna shows good radiation characteristics and obtains a reasonable gain over the entire operating frequency band. The antenna gain varies between 2.7 and 4.32 dB within the operating frequency band of the antenna. The maximum efficiency of the antenna is obtained to be 95.4% at 5.5 GHz.

A comparative study on the different approaches exploited to generate a wide impedance bandwidth with circular polarization is presented (Table 1).

We can highlight the following analytical conclusion based upon the literature and the comparison:

(i) Generally, the operational bandwidth of CP antennas [14] with conventional designs is relatively narrow.

https://doi.org/10.1017/S1759078720000331 Published online by Cambridge University Press

Table 1. Comparative study of different circularly polarized antennas having wide impedance and axial ratio bandwidths

Reference number	Overall dimension (mm^3)	Feed type	Impedance bandwidth	Axial ratio bandwidth	Remarks
[14]	50 × 50 × 1.6	Single feed	4.4%	1.45%	Size Reduction of about 36%
[19]	60 × 60 × 1.6	Single CPW feed	107%	68%	Gain can be enhanced by cavity backing
[22]	82 × 82 × 1.524	Single L-shaped feed	57%	46.5%	Asymmetric structure results high cross-polarization levels for angles other than broadside direction.
[24]	60 × 60 × 0.8	Single CPW feed	51.4%	48.8%	Novel, lightning-shaped feed line is used.
[25]	60 × 60 × 0.8	Single CPW feed	132%	32.2%	Relatively narrow CP bandwidth compared to wide Impedance bandwidth.
[28]	Outer Circumference between 55 mm and 175 mm	Single probe feed	26%	16.3%	Archimedean Spiral structure, enhanced gain of 8.5 dB using reflector backing.
[36]	21.66 × 10.83 × 9.5	Single Aperture feed	36.15%	33.6%	Rotated stacked structure. High gain of 10 dBic achieved.
[39]	180 × 180 × 0.8	Proximity coupled hybrid feed	38%	29.7%	Measured peak gain around 5 dB at the cost of a complex feeding network.
[40]	150 × 150 × 38	Wilkinson's power divider based multiple feed	41%	33%	Bulky structure, complex feed, reasonable high gain of 6.5 dBic.
[42]	110 × 110 × 28	Capacitive-coupled four probe feed	27%	16%	Relatively narrow bandwidth with respect to a significantly bulky structure.
[49]	40 × 39 × 1.6	Single microstrip feed	118.4%	6% (lower band) 23.1% (upper band)	I-shaped slit in the rectangular radiator and I-shaped stub in the ground plane increases the Operational bandwidth of the upper band
[50]	60 × 60 × 0.8	CPW feed	118.2%	62%	Perhaps the first reported work to introduce partial impedance steps for better impedance matching with lower metallization. This in turn increases radiation efficiency.

(ii) Single-fed structures [14, 28] usually have narrow AR bandwidths. However, exceptions are also there as reported in [19, 22, 50, 51].
(iii) By using complicated feeding structures like hybrid feeding [39], power divider networks [40], impedance bandwidth, as well as AR bandwidth can, however, increase at the cost of higher design complexity.
(iv) Operational bandwidth can also be increased by increasing the overall dimensions, possibly by introducing, stacked structures [36], air gaps [42], using cavity backing [19], and using reflectors [28] etc, which might increase the return loss and the AR bandwidth or the gain in some cases, but make the antenna unsuitable for multiple system integration.
(v) Some novelty in the structure has also been observed in [24,28] which reported reasonable performance characteristics.
(vi) The concept of partial impedance steps is introduced in [50], which improves matching greatly, resulting in a wide impedance as well as AR bandwidth, minimizing metallization. The radiation efficiency also increases significantly.

CP dielectric resonator antennas (CP DRA)

DRAs form a domain of very promising radiating elements, particularly for high-frequency applications. Although, in the primitive state of applications, the dielectric resonators (DRs) were used as filters and oscillators i.e. energy storage elements, Richtmyer in 1939 [52] first published a comprehensive article showing that these resonators can also be used as efficient radiators. The first theoretical and experimental analysis of a cylindrical DRA was carried on by Long *et al.* in 1983 [53]. Since then DRA technology has been growing tremendously and has become a focal area for modern wireless communication engineers. A DRA basically consists of a block of dielectric material (especially having high dielectric constant), glued on the top of a patch or a planar monopole over a substrate (of a relatively lower dielectric constant). The antenna may or may not have a ground plane.

DRAs usually use a block of dielectric ceramic as the basic radiating element. So in a way, they reduce metallization, which in turn reduces conduction loss as compared to conventional microstrip antennas. Also the power loss due to surface currents

https://doi.org/10.1017/S1759078720000331 Published online by Cambridge University Press

is minimized. This entitles DRAs to enjoy higher gain, better radiation efficiency and generally higher bandwidth than their conventional microstrip monopole counterpart. Also, depending upon the fabrication of the DR geometry and proper design of the feeding network, different modes can be excited within the DR, and they can be efficiently controlled as well providing design flexibility and result optimization.

In [54], a novel high gain and broadband hybrid DRA is designed and experimentally verified. To obtain the wide impedance bandwidth, the proposed antenna geometry combines the DRA and an underlying slot with a narrow rectangular notch, which effectively broadens the impedance bandwidth by merging the resonances of the slot and DRA. An inverted T-shaped feed line is used to excite both antennas, simultaneously. It supports articulation of different resonant modes of the both, DRA and slot antenna. The proposed antenna offers an impedance bandwidth of 120% from 1.67 to 6.7 GHz. The antenna gain is enhanced by a reflector placed below the antenna at an optimum distance. On optimizing the height and dimension of this reflector the antenna gain is improved from 2.2 to 8.7 dBi at 1.7 GHz.

Mongia *et al.* published a comprehensive review of the modes and the radiation properties of several DRs [55], whereby accurate close form expressions for the resonator frequencies, radiation quality factors and fields inside a DR were also described. Since inception, the volume of research that has continued till recently about DRAs has mostly been reported to have linearly polarized radiation pattern [56–88]. So setting aside the inherent benefits offered by a DRA like enhanced gain and increased radiation efficiency due to low metallization, the operation often gets limited as a result of the linear polarization. This potential difficulty was considered with due concern and as a result of ongoing research saw the introduction of CP DRA. The ability of DRAs to support multiple radiating modes simultaneously is well exploited in the design of CP DRAs.

Design of CP DRAs commenced with [89] that proposed a rectangular DR, with two opposite corners truncated similarly as with a rectangular patch microstrip antenna to produce CP. Mongia *et al.* [90] produced CP by exciting two orthogonal $HE_{11\delta}$ modes of a cylindrical ring DRA using a 3 dB quadrature coupler. In [91], a slot coupled rectangular DRA is used where the DRA position is adjusted to 45° with respect to the slot to produce CP over a bandwidth of 3.4%, and beamwidth of 110°. A design with dual conformal strip feed [92] can also produce CP over a wider bandwidth of 20%. In some designs, backing cavities are used [93] to block back lobe radiation, thereby enhancing the gain of the antenna. A novel structured DRA in the form of a stair-shaped DR fed by a slot is also reported [94], generating CP over a bandwidth of 10.6%. A cylindrical DRA with longitudinal slots of limited depth has been demonstrated [95] to produce CP over just 4% AR bandwidth.

It has been observed that majority of the CP DRAs in literature use either rectangular or cylindrical shaped DRs, though other DR shapes are also used to some extent. The shape of the DR and also the architecture of the feeding network can be optimized to generate requisite modes and thereby radiate circular polarization. Thus, these parameters do offer a great deal of design flexibility for arriving at the desired results. In a cylindrical DRA, one of the major controlling factors for obtaining circular polarization are the aspect ratio, which is the ratio of the diameter to the height of the cylindrical DR [96]. For sectored DRAs [97], the sector angle is also a controlling parameter for circular polarization.

In [98], a two-port fed cylindrical DRA has been proposed for CP operations. It consists of an annular cylindrical DR placed in an open space environment above a circular TMM6 thermoset microwave substrate of dielectric constant 6.15 and thickness of 1.524 mm. The resonator has an outer radius of $R_{DRo} = 8.82$ mm, inner radius, $R_{DRi} = 2$ mm, the height of 7.9 mm, and a dielectric constant of 38. The L-shaped lines are placed at a distance of $d = 5.8$ mm from the center of the resonator. From the latter edges, curved lines of width $w_1 = 0.8$ mm are used. At the 90° phase difference junction, the two parallel 80Ω lines will meet resulting in 40 Ω impedance. Therefore, a quarter-wavelength transformer of width $w_2 = 2.7$ mm can be utilized to obtain 50 Ω impedance at the edge where an SMA connector is connected to form port 1. Figure 7(b) shows the rotation of electric field vectors inside the DR at 3.15 GHz by exciting the port 1 and terminating the port 2 with a matched load impedance, as shown in Fig. 7(a). The corresponding AR bandwidths of the antenna in two orthogonal planes are shown in Fig. 7(c). It can be observed that the electric field lines are not deformed significantly within the resonator due to the existence of the conducting probe inserted inside the resonator, shown in Fig. 7(a). This ensures the polarization purity of the antenna.

A rigorous survey on the various techniques used for designing CP DRAs informs us that circular polarization can be obtained from a DRA using the following methods:

(i) Single-point fed CP DRA [56–72].
(ii) Multi-point fed CP DRA [92, 98–100].
(iii) CP DRA using sequential rotation technique [101–103].
(iv) Slotted or sectored CP DRAs [85, 97].

However, a multi-point fed CP DRAs and sequential rotation method results in designing a feeding network which is relatively more complex and difficult to control optimally, but, if properly exploited by proper mathematical models and sound simulation techniques, may yield impressive results, as already discussed.

Unlike single-point fed CP DRAs, which are simple to fabricate, but typically of narrow bandwidth, multi-point fed DRAs, although structurally complex, may yield wider AR bandwidths. The authors in [99] reported a rectangular-shaped DRA, excited with vertical strips, in combination with a phase quadrature network. As a result of this excitation, multiple CP modes (TE_{111} and TE_{113}) were generated simultaneously in the rectangular DR for an enhanced AR bandwidth. Although, the theoretical resonant frequencies of the fundamental mode TE_{111} and the higher-order mode TE_{113} were found to be different, however, the resonance of these two modes occurred close to each other. In this design, both the modes were generated in the x- and y-directions by placing equal size vertical strips on the two side walls of the rectangular DR. The reported impedance bandwidth of the antenna was 32.8%. The measured AR bandwidth of the antenna was measured to be lying within the entire impedance bandwidth.

Another interesting structure for broadband CP DRA was illustrated in [100]. In this paper, a two-point feed is used in combination with a switched line coupler for exciting a rectangular DR for radiating CP fields. In the structure, a square-shaped DR was placed in the center of a grounded substrate. The resonator was excited by a 3 dB Wilkinson power divider and a wideband 90° phase shifter. The switched line coupler circuit was printed on the front side of the substrate, while the DR was placed on the ground plane. The Wilkinson power divider circuit serves the purpose of equal power division between the different feeding arms and also impedance transformation between the input and the output ports. A couple of quarter wave transformers were

https://doi.org/10.1017/S1759078720000331 Published online by Cambridge University Press

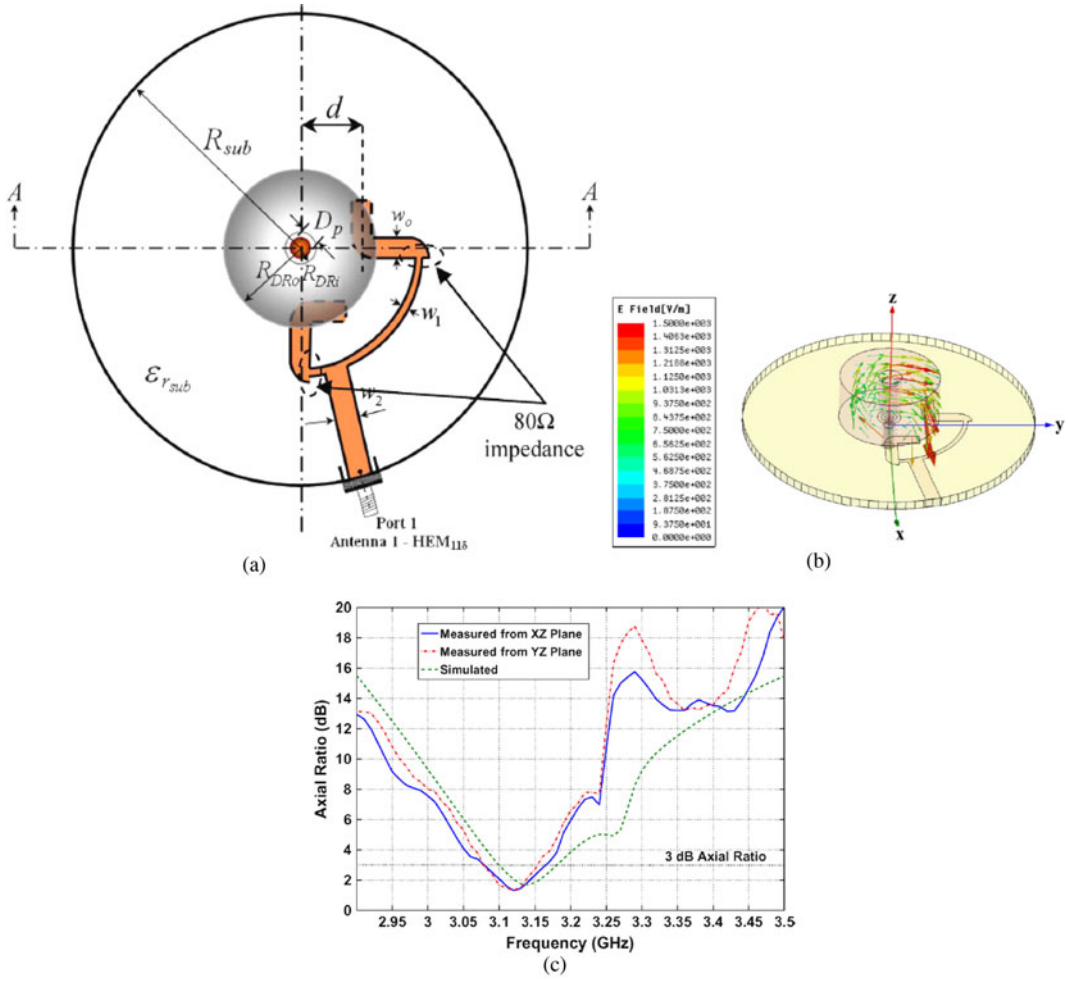


Fig. 7. (a) A circularly polarized DRA showing (a) schematic structure, (b) electric field rotation, and (c) axial ratio bandwidth [98].

used to split the signal from the input port into two different paths and then transmit it, so as to generate a 90° phase difference at the output ports. This structure generates an AP bandwidth of 48% and also stable main beam radiation properties in the broadside of the antenna.

The notable drawback of the two-point fed network, as already has been mentioned, is an increased level of metallization, due to the requirement of additional circuit area for designing the power divider network. Also, the overall antenna architecture is quite complicated. An alternative technique is the sequential rotation mechanism, whether either the feeding network or the antenna elements are rotated sequentially. It is worthy to note here that in this technique, the feeding is necessarily single-point, thus maintaining structural simplicity.

The feeding network for sequential rotation is designed in such a manner that the antenna elements are energized in a progressive 90° phase shift at each excitation point. Several research articles [101–104] showing the use of sequential rotation feeding technique to generate circular polarization in DRA do exist in literature.

In [102], a CP DRA with a metallic strip is reported. The antenna uses a sequential rotation feeding to generate circular polarization. The bandwidth below −10 dB is smaller than the corresponding single element counterpart, which is attributed to the small bandwidth of the feeding network. The measured and simulated AR along the *z*-axis for the array confirms the enhancement of AR brought about by the sequential rotation. In particular, the array exhibits an AR below 1.5 dB over the whole −10 dB matched band, which represents a bandwidth over 18%. Measured losses at 14.6 GHz reach 0.56 dB for the array and are mainly due to the feeding network. The measured and simulated left-handed CP (LHCP) far fields and right-handed CP (RHCP) far fields.

In [103], the authors reported three different types of sequentially rotated fed DRA. In the most commonly used configuration, the feeder shows an input port which is a 50 Ω microstrip line. A few quarter-wave impedance transformers are used to divide the input power into four output ports. The output points are arranged in such a way that each point is located at a distance such that mutual coupling between the resonating elements does not affect the radiation properties. The corresponding output points are excited with a 90° phase shift signal in an anticlockwise sequence. Furthermore, the corners of the microstrip line are chamfered for a smooth transformation of power at the junction discontinuities of the feeding network. The output of the parallel-feed network was coupled to the antenna using probe and slot configuration which yielded AR bandwidths of 26 and 23%, respectively.

Although in this work, the input port is considered to be a 50 Ω microstrip line, but this can only be considered for thin substrates. For thick substrates, 50 Ω line impedances is not

https://doi.org/10.1017/S1759078720000331 Published online by Cambridge University Press

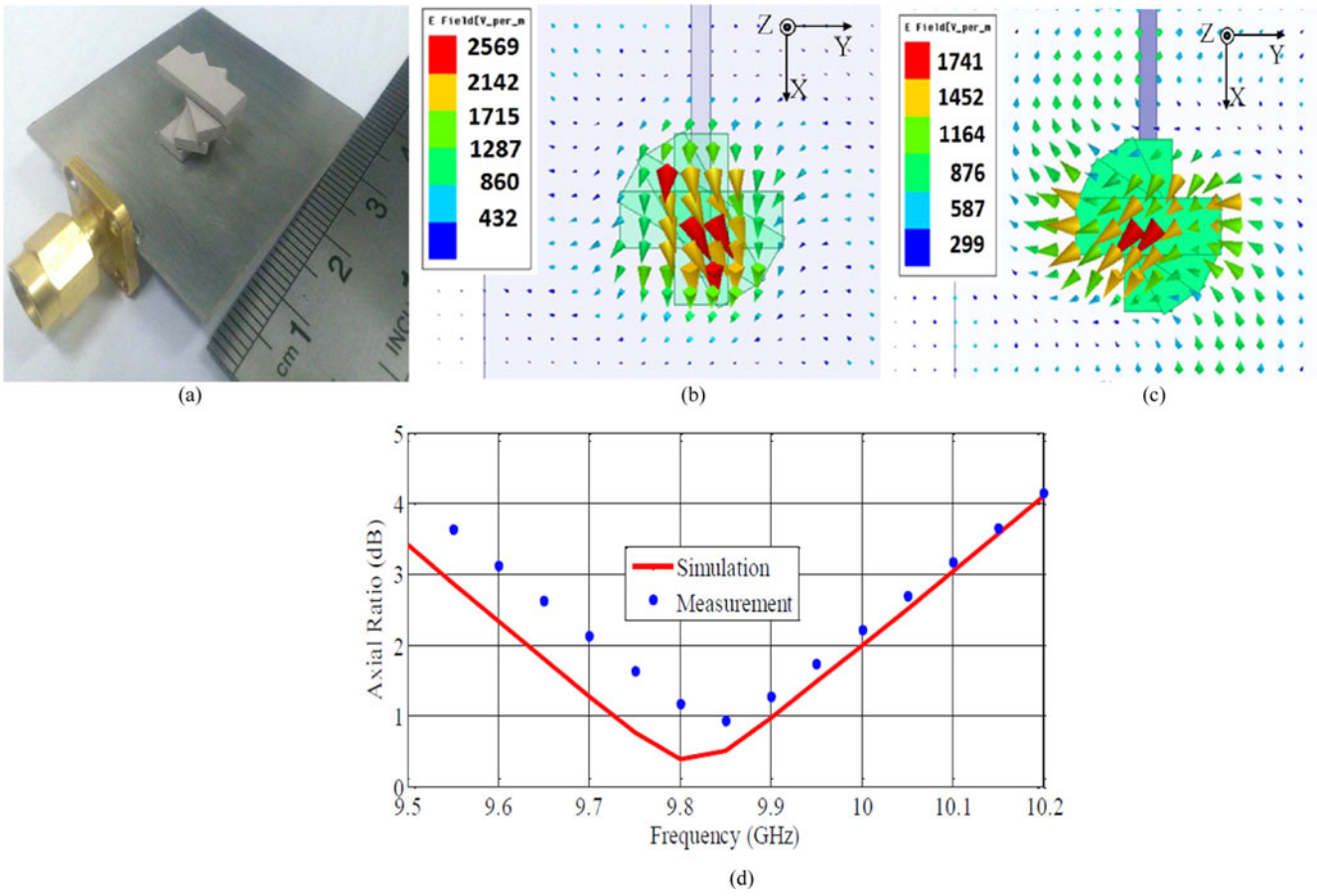


Fig. 8. A CP DRA showing (a) the fabricated prototype, (b) electric field distribution at 9.5 GHz, (c) electric field distribution at 10.15 GHz, and (d) axial ratio bandwidth [104].

recommended as it will increase the coupling in the center of the circuit, which will lead to radiation losses in the feeding network.

It is also indicated from various experimental results that further improvement in the CP DRA can be achieved by using inhomogeneous DRs with special geometries, or by modification of the dielectric characteristics of the common DR shapes in the azimuth direction.

A stacked DRA [104] for CP characteristics is shown in Fig. 8(a). The rotation of the electric field vectors at two frequencies of 9.5 and 10.15 GHz are shown in Figs 8(b) and 8(c), respectively. It is observed from this study that the excited mode is clearly TE^{y}_{111}at 9.5 GHz, since the *E*-field is mostly oriented along the *x*-axis and that TE^{x}_{111} mode excited at 10.15 GHz, since the *E*-field is mostly oriented along the *y*-axis. The corresponding AR bandwidth is shown in Fig. 8(d).

A comparative study for different reported papers on CP DRAs presented. The analysis highlights different techniques used, results obtained and further scope of research (Table 2).

Fractal based CP antennas

According to Mandelbrot [105], fractals are defined as "a rough or fragmented geometric shape that can be split into parts, each of which is (at least approximately) a reduced-size copy of the whole". The major characteristic feature of the fractal geometry is perhaps its "self-similarity" in multiple orders of its iteration. As the order of iteration increases, the structure becomes complex, no doubt, but at the same time, the total length of the fractal progressively increases, keeping the overall peripheral dimensions unchanged (Fig. 9).

A fractal antenna is an antenna that employs the fractal, self-similar design to maximize its effective length or increase the perimeter (on inner sections or the outer periphery) of a material (patch or a monopole) that can receive or transmit electromagnetic radiation, maintaining a given total surface area or volume.

Such fractal antennas are also referred to as multilevel and space -illing curves, but the key aspect lies in their repetition of a pattern over two or more scale orders, or "iterations". For this reason, fractal antennas are usually very compact in nature. They may exhibit multiband or wideband radiation and have useful applications in telephonic communication and other recent aspects of wireless communications. A fractal antenna's response differs remarkably from traditional antenna designs, in that it is capable of operating with good-to-excellent performance at many different frequencies simultaneously [106–109]. Normally standard antennas have to be physically sized for the resonant frequency meant for their use and thus the standard antennas only work satisfactorily at that frequency.

A novel design, based upon a modified Koch fractal geometry has been designed for achieving circular polarization with a square radiator by creating a pair of asymmetric Koch fractal geometries on the *x*- and *y*-planes of a single probe feed [110]. A defected ground structure (DGS) is designed based upon fractal geometry for improving antenna characteristics like operational

https://doi.org/10.1017/S1759078720000331 Published online by Cambridge University Press

Table 2. Comparative study of different circularly polarized dielectric resonator antennas (CP DRAs)

Reference number	DR dimension [each component in (mm)]	Feed type	Impedance bandwidth	Axial ratio bandwidth	Observations
[90]	External diameter = 11.95 Internal diameter = 2 Height of DR = 4.5 Length of probes = 7	3 dB quadrature coupler assembly	66.7%	11%	Quadrature coupler feeding technique is used, which is relatively complex.
[91]	14 × 3.7 × 3.24	50 Ω microstrip line through a single aperture	1.4%	3%	Relatively simple structure but a very narrow bandwidth.
[92]	100 × 100 × 11.6	Dual conformal strip feed	13.7%	20%	A complex feeding structure using 90° hybrid coupler making overall structure bulky but enabling direct integration with MMICs.
[93]	DR radius = 20 DR height = 20	Coaxial feed with a perturbed annular slot	18%	3.4%	The authors claim that a backing cavity used enhances the gain to achieve a peak value of 4.5 dBi.
[94]	18.34 × 9.66 × 5.2	Microstrip line fed, slot coupled	36.6%	10.6%	Novel, rotated stair-shaped DR, with good cross-polarization discrimination of over 15 dB.
[99]	DR dimension = 18 × 18 × 29 Ground Plane = 205 × 205	Quadrature fed	32.8%	36.9%	Simple structure with dual mode operation. Gains of the two CP modes are 2.1 dB and 6.1 dB respectively, which are quite appreciable.
[100]	DR dimension = 9.8 × 9.8 × 9 Ground Plane = 42 × 42 × 0.5	Wideband switched line coupler comprised a 3 dB Wilkinson Power Divider and a wideband 90° phase shifter	48.46%	47.69%	Comparatively complex feeding structure, provides a decent operational bandwidth and a significantly high gain of 6.4 dB.
[102]	DR dimension = 5.25 × 5.25 × 2.5	Microstrip line fed, slot coupled	30%	6%	Extension of the structure to a 4 element array fed by sequential rotation enhances the axial ratio bandwidth to about 18%.

bandwidth, cross-polarization levels and gain in [111]. Planar CP fractal antennas have been extensively studied and reported in the literature for WLAN applications [112] owing to their compact dimensions.

In [112], iteration factor (IF) is also varied to study the performance of the antenna. The novel motive of this work is bringing out the link between the IF and the AR bandwidth for the design of a broadband antenna, proving that IF is also an influential parameter in fractal CP antenna design. The method used in this paper is a hybridization of fractal structure and diagonal slots. A broadband response is achieved compared to conventional diagonal slot design (Fig. 10).

Further, for GPS applications, a circular patch cross-over module has been reported in [113]. A CP fractal antenna for GPS system using a modified and optimized Minkowski fractal structure has been demonstrated in [114].

A popular method to obtain circular polarization using fractal geometry is employing DGS [115–118], which are tactically etched portions from the ground plane, which can perturb the surface current distribution on the ground plane. By embedding the DGS, the field of one mode of the excited field vector can be made to lead by 45° while that of the other can lag by 45°, resulting in a 90° phase difference necessary for circular polarization. Thus as DGS increases the AR bandwidth for circular polarization [118].

In [119], the methodology proposed is to replace the straight sides of the square patch by different fractal curves. Because of this slight difference in electrical length in two mutually perpendicular directions of the patch, two spatially orthogonal modes are excited. By effective dimensional tuning of the fractal curves, compact CP fractal microstrip antennas can be realized. In addition to the generation of CP, it is always possible to attain structural miniaturization.

In [120], a single probe-fed singly layer antenna is proposed. The antenna design is based upon Minkowski and Koch fractal geometries. The antenna shows tri-band radiation characteristics with impedance bandwidths 12.7, 2.52, and 7.5% respectively, while exhibiting AR bandwidths of 1.53, 0.81, and 1.62%, respectively. The proposed antenna is suitable for WLAN and WiMAX applications.

In recent works, the concept of fractal geometries in the microstrip antenna design has been incorporated for multiband, wideband, and size reduction [121, 122]. Tri-band CP radiation was achieved by using asymmetrical Koch fractal curved boundaries and embedding rectangular slot in a square patch structure [121]. The behavior of the Koch fractal-based monopole is numerically and experimentally analyzed to show that the quality factor of the antenna approach to the fundamental limit for geometrically small antennas, as the number of iterations is increased on the small fractal Koch monopole [122].

In [123] a unique method is proposed to obtain decent circular polarization using a fractal curve as the boundary of the antenna. This is achieved by choosing a proper fractal shape and dimension in each side of a square patch while keeping the dimension constant for the opposite sides. The length of the fractal curve can be effectively tuned by altering the fractal dimension.

https://doi.org/10.1017/S1759078720000331 Published online by Cambridge University Press

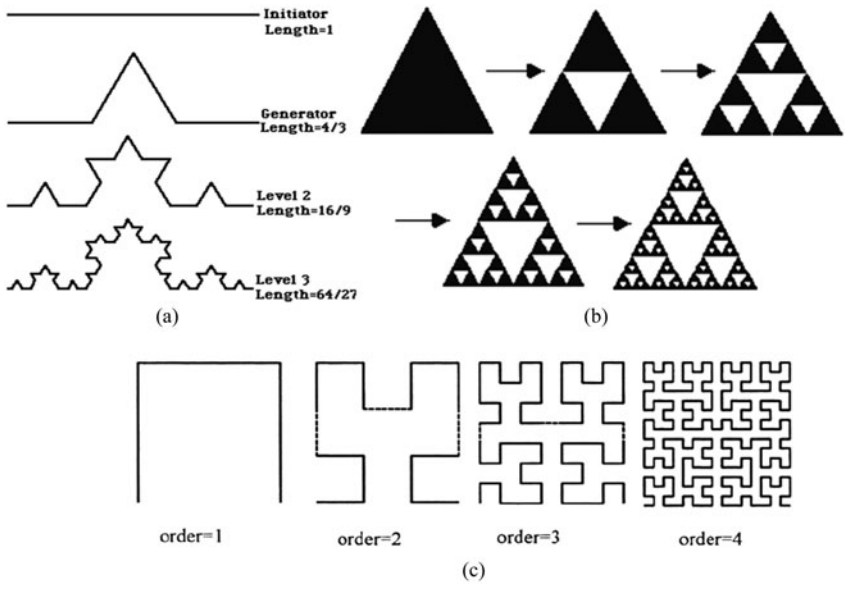


Fig. 9. Different fractal structures like (a) Koch Snow flake (b) Sierpinski Carpet, and (c) Hilbert Fractal [105].

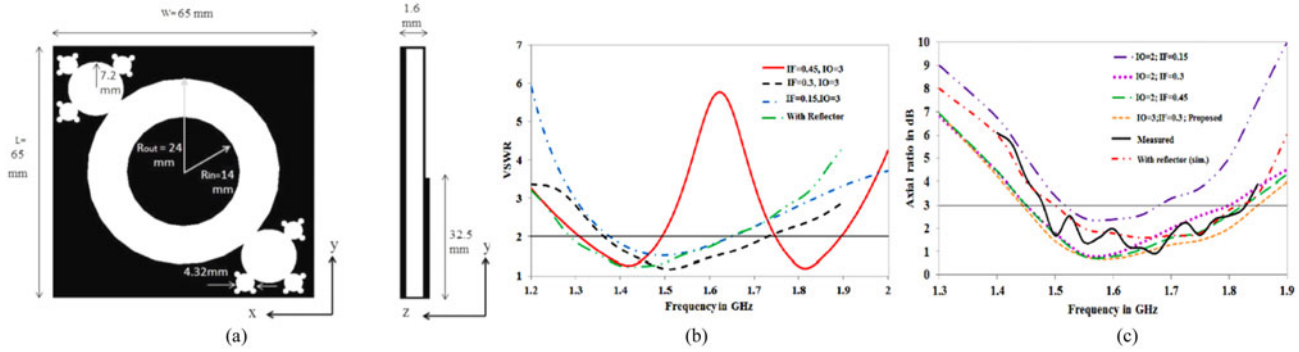


Fig. 10. The (a) structure of a CP fractal Antenna and its (b) VSWR, and (c) axial ratio Bandwidth [112].

Circular polarization, as previously mentioned, can be obtained when two orthogonal modes with equal amplitudes, which are excited within the patch. This is possible by choosing different electrical lengths in two directions of the patch. When a Koch curve with a different indentation angle is used as the boundary for the square patch, its electrical length varies since the length of the Koch curve is a function of indentation angle. The length of the *n*th iterated Koch curve can be expressed as:

$$L_n\left(\frac{4}{2(1+cos\theta)}\right)^n L, \tag{3}$$

where, n = iteration number, L = initial length of the curve, L_n = length of the curve after nth iteration, θ = indentation angle.

The fractal dimension of the Koch curve in terms of the indentation angle is given as

$$D = \frac{\log N}{\log s}, \tag{4}$$

where, $s = 2(1 + \cos\theta)$ = scaling factor, D = fractal dimension, N = number of segments.

So, in this paper, the concept of varying the fractal dimensions of the boundary is employed to achieve different electrical lengths in two directions of the patch, which in turn excites two orthogonal modes necessary for circular polarization.

The Jerusalem cross (JC) is another notable fractal model used in a number of researches for increasing antenna gain and bandwidth enhancement [124, 125]. In addition, the slot antenna has been studied to achieve circular polarization with a change in slot feeds and parasitic elements in some researches [126–131]. Slot antennas with various techniques for obtaining circular polarization are implemented, such as square-ring slot antenna fed with an L-shaped coupling strip [127], dual-square ring-shaped slot [128], and two-slot rings [129]. Coplanar waveguide (CPW)-fed slot antennas such as two asymmetrical C-shaped strips [130] and corner-truncated ground [131] are also noticed for the feasibility of achieving circular polarization.

In [132] a fractal JC slot antenna is designed for circular polarization. For this aim, a special shape of the slot, a broken cross shape is used to alter the antenna's surface current distribution to achieve circular polarization. In addition, a T-shaped feed line is used to increase the effective length of the antenna for miniaturization and saving symmetrical formation of the antenna for obtaining circular polarization, and a triangular slot in feed line is used for improving the antenna's impedance matching. In addition, by varying the length of the feed line, a fair control of the coupling to the ground plane is achieved and therefore

https://doi.org/10.1017/S1759078720000331 Published online by Cambridge University Press

the best length for matching has been attained. At last, the JC slot is implemented on the ground plane.

In [133] a multiband CP antenna is introduced using the novel square and Giuseppe Peano fractals. It is designed for operation in, Global positioning system L1 (GPS 1.575 GHz); Hiper-Lan2 (High Performance Radio Local Area Network Type2) in the band 2.12–2.32 GHz; IEEE802.11b/g in the band from 2.4 to 2.484 GHz, which is one of the WLAN bands and IMT advanced system or fourth-generation (4G) mobile communication system in the band 4.6–5.2 GHz. The miniaturization and multi-banding [134] properties of the square fractal microstrip patch antenna is also investigated and presented (Table 3).

Metamaterial based CP antennas

Metamaterials are structural units typically designed with novel or artificial components to generate electromagnetic properties that are unusual or difficult to be obtained in nature. This concept is incorporated in designing antennas [135–143] during the last few decades. Metamaterial antennas are a class of antennas involving metamaterials to enhance their capability or to achieve novel functions. They can be classified as leaky-wave antennas [135] and resonator type antennas [136]. Metamaterial-based antennas may also be based upon meta-resonators [136] and/or metamaterial loadings [137]. These antennas have distinguished benefits like small physical dimensions, low cost, wide bandwidth, and good radiation efficiency.

It is pre-postulated that the quality factor and the radiation loss of the antennas are inversely related to the antenna size [138]. Metamaterial-based small antennas are proposed [139] for providing means to manipulate the near field boundary conditions which could contribute to antenna miniaturization, maintaining good radiation performance. Metamaterial-based antennas have enlightened researchers to overcome the restrictive efficiency-bandwidth limitation for small antennas [140].

In [141], a coaxial probe-fed cylindrical DRA is proposed that obtains an impedance bandwidth of 0.9% and an AR bandwidth of 0.4%. The antenna uses the zero-order resonator (ZOR) mode of epsilon negative (ENG)-based transmission line to obtain the omnidirectional radiation pattern and the vertical polarization. Also, the horizontal polarization is achieved by the curved branches. The gain obtained is low, about −0.4 dBic.

Metamaterial-based antennas, nowadays, are extensively used for the design of CP antennas. Various metamaterial-based CP antennas are reported in [135–143], some of which use complimentary split-ring resonators (CSRR) [142], 2×2 mushrooms [143], fractal resonators [144], ENG-based transmission line-based annular rings [145], sector-shaped circular array [146]. In these reported antennas, it is observed that they suffer from narrow impedance bandwidth, narrow AR bandwidth, poor gain, comparatively higher design complexity, bulky size etc.

In [144], the concept of Wunderlich-shaped fractal complementary split ring resonator (WCSRR) is introduced. Figure 11 (b) shows the electric field distribution at 3.5 GHz in time-domain. A clockwise rotated electric field moving along the patch edge is observed, indicating the LHCP nature. Progressive research indicates that RHCP antenna can be designed by mirroring the WCSRR structure to the right part of the patch. In addition, the discrepancy of the electric field on WCSRR at different stages also justifies that the slot is essential in exciting the CP wave. The AR bandwidth is significantly improved for the antennas with Meandered line-loaded complementary split ring resonator (MCSRR) and WCSRR loading.

Metamaterial-based antennas are suitable radiators for the design of miniaturized low profile antennas. Metamaterials based on composite right/left-handed (CRLH) structures which offer negative or ZOR modes, which can be used for the design of miniaturized antennas [147, 148].

In [149], a somewhat better solution with improved impedance bandwidth is presented. The proposed antenna is also relatively compact, low profile, and ENG-based transmission line-based CP metamaterial antenna. The measured impedance bandwidth of this antenna is 10.86%. Although the authors claim that this antenna performs better in comparison to the previously mentioned structures, the AR bandwidth obtained in this structure is only 2.54%.

In [150], a dual-band CP antenna, based on the principle of CRLH transmission line has been reported. In this structure, two separate power divider networks provide 90° phase shift between the two input ports. The antenna has dual bands at 1.768–1.776 GHz and 3.868–4.007 GHz i.e. 0.5 and 3.6% impedance bandwidths, respectively. The AR bandwidths range from 1.772 to 1.779 GHz and 3.953–3.972 GHz i.e. 0.39 and 0.48% AR bandwidths, respectively. Despite being the fact that the antenna has significantly narrow operational bandwidths, for both the bands, it can generate about 70% beam width for 3 dB level and has a decent peak gain of about 2.5 dB for both the bands.

Presently, vast attention is paid to research and development of chiral metamaterials due to their attractive electromagnetic properties [151]. In this type of metamaterials, the degeneracy of the two CP waves is broken i.e. refractive index for the RHCP and LHCP waves are different [152]. Thus the RHCP and LHCP waves would have different transmission coefficients at the resonances. In [153], the chiral metamaterial concept is used to achieve RHCP and LHCP radiation at 6.4 and 8.1 GHz, respectively. The measured co-polarization and cross-polarization discrimination exceed 40 dB at the resonant frequencies, which is quite appreciable. The proposed structure based on bi-layer, twisted split ring resonator (SRR) approach can be made to exhibit dual-band or multiband operation by combining different sized twisted SRR structures. In addition, the proposed structure can also be operated at other specific high-frequency bands such as Terra-Hertz frequency range or even optical frequency range by downscaling geometrical dimensions.

Thus the review can summarily comment that when integrated with monopole or microstrip patch antennas, such metamaterial structures can improve different performance aspects such as provide gain enhancement [154, 155], side lobe and back lobe reduction [156], antenna dimension miniaturization [155, 157], improve radiation efficiency [158], support dual-mode operation [159], and/or enable impedance bandwidth broadening [157].

A comparison table is provided which highlights some of the existing metamaterial-based CP antennas in the literature, with the motive to contribute to the vastly developing advanced domain of CP antennas (Table 4).

Multiband CP antennas having novel structures and band-specific applications

Due to the enhanced system requirements of modern wireless communication applications, multiband CP antennas with structural compactness and broad bandwidth draw significant attention [160]. Also to cater to different specific bandwidth ranges,

https://doi.org/10.1017/S1759078720000331 Published online by Cambridge University Press

https://doi.org/10.1017/S1759078720000331 Published online by Cambridge University Press

Table 3. Comparative study of different circularly polarized fractal antennas

Reference number	Overall dimension (mm^3)	Feed type	Type of fractal Used	Impedance bandwidth	Axial ratio bandwidth	Observations
[110]	54 × 54 × 1.6	Single probe feed	Koch Fractal	0.8%	0.4%	The proposed structure has a relatively high peak gain of 5.85 dB.
[111]	45 × 45 × 3.18	Single probe feed	Fractal Defected Ground Structure	2%	0.4%	The third order iterative Fractal DGS makes the structure complex. Moreover, the operational bandwidth and the peak gain of 2.2 dB are quite low.
[112]	65 × 65 × 1.6	CPW feed	Hybrid fractal structure with diagonal slots	25.4%	21.8%	Although structurally complex, the antenna has a significantly high gain of 6.6 dB. The efficiency is also as high as 94%.
[114]	55 × 55 × 1.6	Single probe feed	Minkowski Fractal	3.7%	2.8%	The authors claim that the antenna can be used in Satellite communication and GPS applications
[119]	90 × 90 × 3.2	Microstrip line fed	Koch curve Fractal with Defected Ground Structure	9.27%	2.1%	The antenna has a high gain of about 5.5 dB. It finds applications in L-band communication and Satellite Communication.
[120]	50 × 50 × 3.2	Single probe feed	Minkowski and Koch Fractal	Triband: 12.7%; 2.52%; 7.5%	Triband: 1.53%; 0.81%; 1.62%	Having Triband radiation characteristics thus catering to WLAN and WiMAX applications. Simple, single-layered structure.
[121]	36 × 36 × 3.2	Single probe feed	Koch Fractal	Triband: 8.7%; 2.4%; 5.0%	Triband: 3.2%; 1.6%; 3.0%	Asymmetric Koch fractal is used. Proposed antenna exhibits WLAN and WiMAX applications. Rotated fractal slot is used for better performance.
[123]	36.4 × 36.4 × 3.2	Single probe feed	Koch Fractal curve	6.2%	1.6%	Size reduction of over 25% is achieved. Although the obtained bandwidth is quite low, the authors have presented a well-structured mathematical model for the design.
[132]	40 × 40 × 1.6	T-shaped microstrip line feed	Jerusalem Cross Fractal slot	23.5%	0.6%	Novel fractal design, obtains a decent gain of 3.5 dB, but at the cost of a very narrow CP bandwidth.
[133]	30 × 30 × 1.6	Two feeding points with electromagnetic coupling	Giuseppe Peano Fractals	Triband: 4.7%; 30.7%; 6.2%	Triband : 6.8%; 1.4%; 1.8%	The antenna achieves significant structural miniaturization and also wide operating bandwidth with lower number of iterations than other conventional fractal structures.

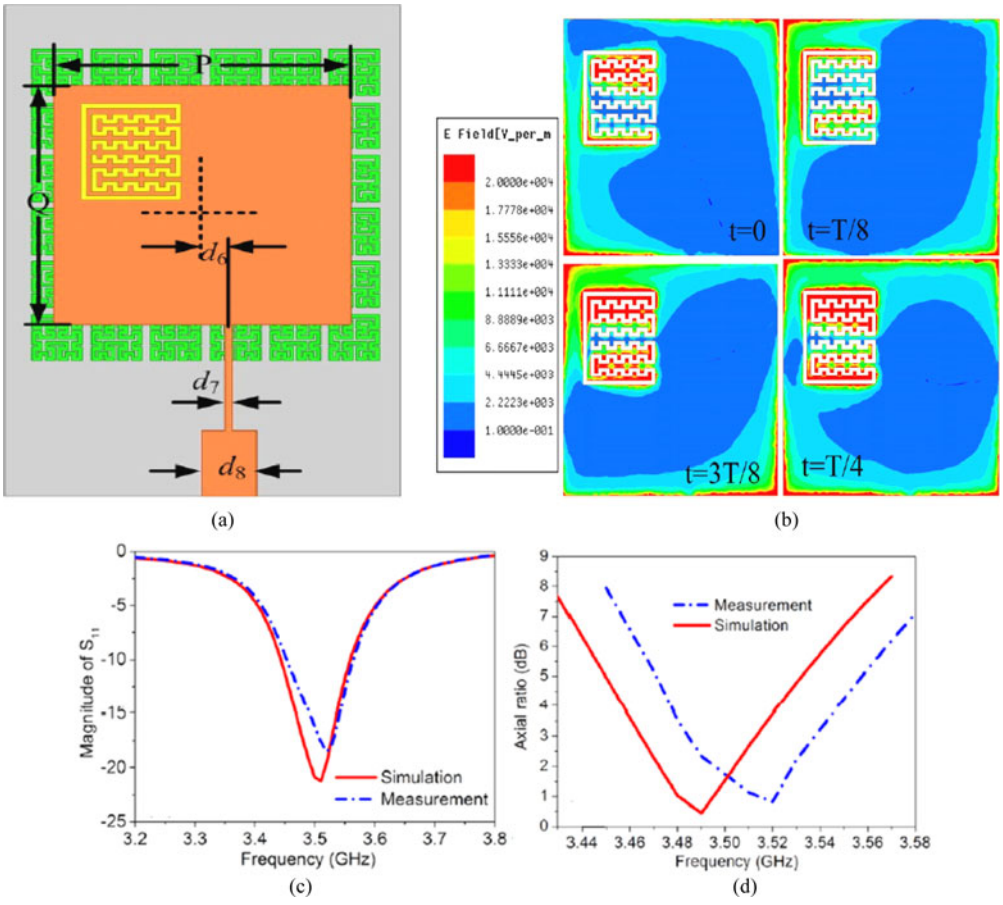


Fig. 11. The (a) structure of a metamaterial-based CP Antenna and its (b) electric field distribution at 3.15 GHz, (c) S_{11} bandwidth, and (d) axial ratio bandwidth [144].

multiband antenna technologies with CP radiation pattern are in prominence [131, 160–196]. In [161], an antenna with a "T" shaped slit and an annular patch exhibits AR bandwidths of 4.02, 4.51, 1, and 12.74% at different operating bands. It is observed that though multiband, the AR bandwidths at the different operating bands are quite narrow. To overcome this, many broadband antennas with multiband CP characteristic feature are proposed [162, 163]. In [162], dual-band, dual-sense CP square slot antenna presented. For enhancing the CP operational bandwidth, an artificial magnetic conductor (AMC) or metasurface is successfully applied in a number of designs [164–166]. AMC can reduce the antenna physical dimensions and significantly enhances the CP operational bandwidth. However, this design approach makes the antenna structure complicated and hence unsuitable to be applied to integrated devices. Using parasitic patches in conjunction to the radiating patch is an effective solution to this problem [167]. In [167], an enhanced dual CP broadband antenna using C-shaped parasitic patch is reported. The overall length of the patch is about half wavelength corresponding to the resonant frequency of the lower band at 4.9 GHz.

In [168], a low profile dual-band antenna for indoor/outdoor wearable applications is proposed. This antenna achieves about 63.86% size reduction related to a convention CP slotted patch antenna [169], and about 15% as compared to other electromagnetically coupled CP antenna designs [170, 171]. This antenna [168] uses a CSRR for size reduction and also to enable CP properties in the lower band. Further, to improve the gain and the front-to-back ratio (FBR) of the antenna, a compact and multiband AMC unit cell is used. As a result, a gain improvement of upto 3.47 dBi and an increase in the FBR upto 21.88 dB in the lower band and upto 22 dB in the upper band was obtained, which is quite appreciable.

In [172], a quad-band printed antenna is proposed for GPS (1.575 GHz), LTE (2.7 GHz), WiMAX (3.5 GHz), and WLAN (5.8 GHz) applications. The antenna uses a combination of four meandered lines which makes the AR bandwidth easily tunable. The authors have also demonstrated that the proposed antenna is suitable for Internet of Things (IoT) applications.

In [173], a wideband monopole antenna has been proposed for applications of multiple system integration. The antenna achieves dual-band CP radiation with a triple sense topology. Although the AR bandwidths obtained are very narrow, yet the authors claim that the antenna can be used for GPS and SDAR bands, where LHCP and RHCP radiation are obtained, respectively.

In [174], a dual-band CP planar monopole antenna has been reported for WLAN/WiFi applications. The monopole radiator consists of a C-shaped strip and an L-shaped strip which are found to be responsible for the upper and the lower CP bands, respectively. The antenna structure is relatively simple.

In [175], a novel, dual-band CP CPW fed slot antenna is reported, which achieves a small frequency ratio and wide CP bandwidth simultaneously. The design is based on the idea of using two simple monopoles to generate dual-band operations [176]. The authors, in this work, have used two deformed parallel

https://doi.org/10.1017/S1759078720000331 Published online by Cambridge University Press

Table 4. Comparative study of different metamaterial-based circularly polarized antennas

Reference number	Overall dimension [each component in (mm)]	Feed type	Impedance bandwidth	Axial ratio bandwidth	Observations
[136]	26 × 26 × 1.9	Coaxial probe feed	8.18%	3.3%	A novel, complementary crossbar fractal tree (CCFT) slot and three-turn complementary spiral resonators (TCSRs). The achieved gain is over 4.5 dBic.
[141]	Outer Diameter = 56 Inner Diameter = 40 Substrate thickness = 3.175	Coaxial probe feed	0.9%	0.4%	Structure is quite complicated and the gain obtained is also quite low, about –0.4 dBic.
[143]	60 × 60 × 3.17	Coaxial probe feed	Lower band = 2.9% Upper band = 0.6%	Lower band = 0.7% Upper band = 0.18%	Although the proposed structure provides a very narrow operational bandwidth, the peak gains of 6.26 and 6.97 dBic are measured at lower and upper bands, respectively. Also, radiation efficiencies of 82 and 65% are measured at each band, respectively.
[144]	40 × 40 × 2.5	Microstrip line feed	3.77%	1.86%	In this structure, the HRIS structure and the WCSRR are applied for designing the miniaturized CP antenna. This together with CSRR structures achieve the CP performance.
[149]	20 × 20 × 2.1	Coaxial probe feed	10.86%	2.54%	The authors claim that novelty of the proposed antenna is its compactness and low profile with wide bandwidth.

monopoles, one curved and another fork-shaped monopole in the feeding line. Moreover, a crane-shaped strip is used as a perturbing element to excite CP radiation. However, the authors have used quite a few structural components only to obtain impedance bandwidths of 17 and 21% and AR bandwidths of 9 and 11% in the lower and upper bands, respectively, which are significantly narrow, compared to the structural complexity involved. The frequency ratio of the upper band to the lower band is 1.286.

The concept of fractal geometry has also been incorporated to obtain multi-band CP radiation. Generally, the CP antennas employing fractal architecture have very narrow operating bandwidth. In [177], two symmetrical fractal structures etched out of a square patch yields decent results in terms of the AR bandwidth. The CP AR bandwidths obtained are 35 and 30%, respectively, in the first and second operating bands. The designed antenna is quite compact in volume and suitable for WiFi (2.4–2.65 GHz) and WiMAX (4.8–6.4 GHz) applications.

A novel, tilted D-shaped monopole antenna with wide dual-band and dual-sense circular polarization is proposed in [178]. The tilted D-shaped design is obtained by combining a tilted I-shaped and inverted C-shaped structures, which are capacitively coupled with each other. The antenna yields a wide impedance bandwidth of 104.5% and AR bandwidths of 31.16 and 22.6% in the two operating CP bands, ranging from 4.28 to 5.86 GHz and from 7.49 to 9.4 GHz, respectively. Cross-polarization discrimination better than 20 dB is observed over the entire operating band.

Another novel structure, nomenclated as CP complimentary antenna has been reported in [179] to exhibit dual-band operation. The antenna consists of a semicircular monopole fed by a 50 Ω microstrip line and the complementary metal is attached to the ground plane on the other side of the substrate. Further, rectangular and L-shaped adjustable stubs are added to the complementary monopole structure to obtain dual-band circular polarization. This antenna is considerably smaller than other contemporary stacked patch antennas and also has a simple feed architecture. However, the AR bandwidths of the two bands are quite narrow, about 1.6 and 11.8%, respectively.

A square slot antenna having triple wideband, triple sense CP radiation pattern is reported in [180]. The antenna consists of an L-shaped radiator and a frame, a lower ground structure with a couple of rectangular strips at opposite corners. A rectangular slit cut out of the rectangular strip at the lower right ground plane is primarily responsible to broaden the AR bandwidth at the upper band. The antenna radiates RHCP in the lower and the upper bands having AR bandwidths of 35.9 and 6.3%, respectively, while it radiates LHCP in the middle band having an AR bandwidth of 44%. The measured peak gains are, respectively, 4.2, 3.7, and 3.5 dBic in the lower, middle, and upper CP bands. This antenna is a promising candidate for WLAN and X-band applications.

Polarization diversity has been an effective way for performance enhancement of adaptive multiple-input-multiple-output (MIMO) systems and also cognitive radio systems [181]. A reconfigurable CP antenna plays a substantial role in increasing the system capacity in a strong multi-path environment. In due course of the research, a number of polarization reconfigurable CP antennas are reported [182, 183]. In slot antennas, polarization can be switched by changing their port of excitation [184]. In [185], PIN diodes are used to attain polarization reconfigurability. However, most of the reported reconfigurable antennas have a single operational bandwidth and hence are unsuitable for systems exhibiting multiple band-specific applications.

A solution to this problem has been achieved in [186], where a microstrip line fed, polarization reconfigurable dual-band, dual-sense CP antenna are presented for WLAN applications. The

https://doi.org/10.1017/S1759078720000331 Published online by Cambridge University Press

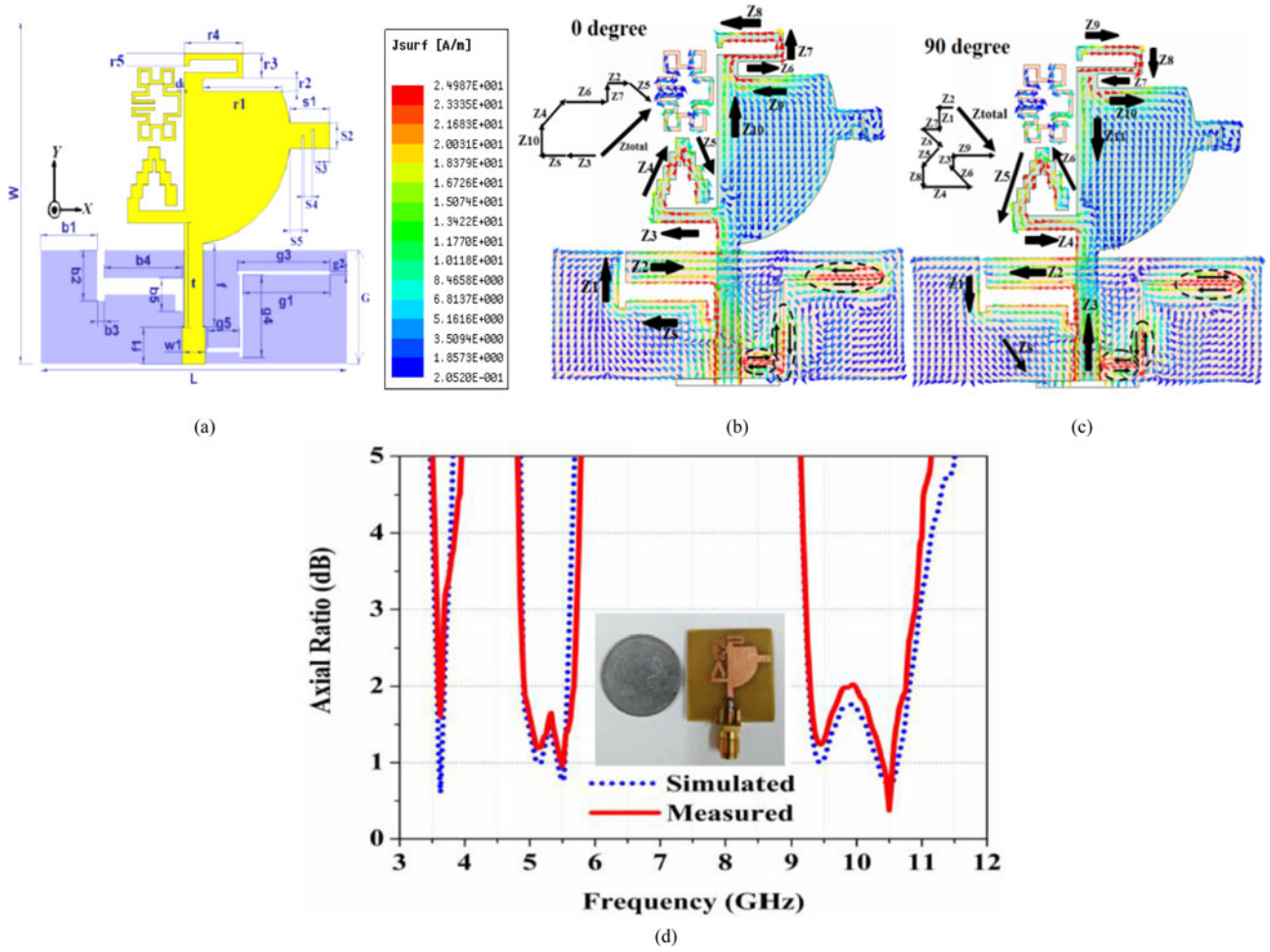


Fig. 12. The (a) structure of a multi-band CP Antenna and its (b) current distribution at 5.52 GHz at 0° phase, (c) current distribution at 5.52 GHz at 90° phase, and (d) axial ratio bandwidths [197].

antenna radiates LHCP in one of the bands and RHCP in the other band. Four PIN diodes are placed on the feed line, whose switching states can be controlled to interchange the sense of polarization. This is presumably the first reported approach to generate dual-band, dual-sense CP reconfigurable antenna. The obtained AR bandwidths are 16.6 and 5.7% in the two bands, respectively.

The signals received from an antenna at different frequencies have to be separated by passing the signals through duplexers and filters for facilitating the functionality of the terminal communication equipments. For maintaining system volume and to reduce architectural complexity, it is worthy to integrate the duplexers, bandpass filters, and other interfaces into the antenna design [187]. In [188], a low-profile, single radiator, dual-band, dual CP patch antenna with integrated duplexing and filtering mechanisms is studied. The lower and upper bands were found to radiate LHCP and RHCP, respectively. In this structure, two hair-pin resonators attached to the feed serve as frequency-selective devices for enhancing the channel isolation. The channel isolation has been profoundly improved by more than 8 and 20 dB, respectively, in the lower and upper band. The measured impedance bandwidths of the lower and upper bands are respectively, 4.7 and 7.3%, while the AR bandwidths of the corresponding bands are 1.1 and 3.2%. A stable gain as high as 8 dBi is obtained in the upper band, while the peak gain for the lower band is 6 dBi. Although the operating bandwidths are quite narrow, the article presents a classic example of multiple system integration within the same antenna structure.

Another simple structure of a single feed, tri-band CP annular slot antenna is presented in [189]. The antenna is fed by L-shaped series step impedance feed configuration. The frequency ratio of the antenna can be tuned by adjusting the dimensions of the two annular slots etched out if it is monopole. The compact structure successfully operates in the L1 and L2 bands of the GPS and the frequency band of the Compass Navigation Satellite System (CNSS). The measured 3 dB AR bandwidths are 7.3, 1.2, 5.5%, respectively, in the three operating bands. The antenna also exhibits consistent gains of 4, 4.6, and 5.7 dBi at the lower, middle, and upper bands, respectively.

In [190], the authors have developed a multiband, monopole, mobile phone antenna, whose operating frequency band covers several wireless communication systems like GSM (880–960 MHz), DCS (1710–1880 MHz), PCS (1850–1990 MHz), UMTS (1920–217 MHz), WiBRO (2300–2390 MHz), ISM (2400–2483 MHz), GNSS Compass (1559.052–1591.788 MHz), GPS (around 1575.42 MHz), and GLONASS (1602–1615.5 MHz). The operation of the antenna is also explained with the help of equivalent circuit modeling. The antenna exhibits good, omnidirectional radiation pattern over the entire frequency range. The proposed antenna has a peak gain of 2.7 dB and overall efficiency of more than 80%. Such an antenna is immensely useful for modern

https://doi.org/10.1017/S1759078720000331 Published online by Cambridge University Press

Table 5. Comparative study of different circularly polarized antennas having multiband response and/or structural novelty

Reference number	Overall dimension (mm^3)	Feed type	Impedance bandwidth	Axial ratio bandwidth	Observations
[160]	25 × 25 × 1	Microstrip line	87.7%	65.2%	Placing a reflector underneath the antenna, an enhanced gain of 6.1 dBi is obtained.
[161]	27 × 27 × 1	Microstrip line feed	150%	Quad-band with bandwidths of 4.02, 4.51, 1%and 12.74% respectively.	The quad-sense CP wave is achieved by a Defected Ground Structure embedded with a T-shaped slit (TSS) and an annular patch etched by an X-shaped slit (XSS).
[165]	50 × 50 × 0.5	Multi-port probe feed	19.6%	15.3%	The structure is based on polarization rotation artificial magnetic conductor (PRAMC) structure. In addition, a switchable network is designed using RFIC switches achieves requisite performance
[167]	60 × 60 × 0.8	CPW feed	117.3%	Dual band: 32.2 and 3.8%	The article proposes an enhanced dual CP broadband antenna using C-shaped parasitic patch (CSPP) for wider bandwidth and enhanced CP characteristics.
[168]	70.4 × 76.14 × 3.11	Y-shaped Electromagnetic coupled Feed line	Dual band: 1.84 and 0.736%	0.83%	The measured gain of the structure is found to be 5.03 dBi in the lower band and 5.07 dBi in the upper band.
[177]	18 × 18 × 0.8	Dual microstrip line feed	Dual band: 4%; 21.5%	Dual band: 4%; 5.1%	The obtained notched bands for the proposed antenna cover all WLAN/ Wi-Fi standards of 2.4–2.484/5.15–5.825 GHz and WiMAX standards of 2.5–2.6/5.25–5.85 GHz. The peak gain is 2.7 dB while the maximum efficiency is 85%.
[180]	60 × 60 × 1	Microstrip line feed	Dual Band: 44%, 70.9%	Triband: 35.9%; 44%; 6.3%	Triple-band, triple sense CP radiation is achieved. Measured gains in the three bands are 4.2, 3.7, 3.5 dB, respectively. The radiation pattern is bidirectional.
[189]	95 × 93 × 0.813	Microstrip line feed	Triband: 9%; 2.5%; 27%	Triband: 4.8%; 1.2%; 3.9%	This antenna covers the L_1 and L_2 bands of GPS and the operating band of CNSS. The measured gains in the three bands are 4 dB, 4.6 dB and 5.7 dB respectively.
[190]	110 × 50 × 1.6	Microstrip line feed	Triband: 30.2, 11.6, 41.6%	5.6%	The antenna finds applications in the GSM, DCS, PCS, UMTS,WiBro, ISM, GNSS, COMPASS, GPS, GLONASS. The measured maximal LHCP and RHCP gain of more than 2.7 dBic. Within all the operating bands, the efficiency is near 80%.
[197]	27 × 27 × 1	CPW feed	112%	Triband : 6.09%; 15.35%; 16%	The monopole shape is novel, being of quad-circular shape. Peak gain is 4.77 dB, while the maximum radiation efficiency is 93.5%.

wireless communication systems by accommodating multiple wireless channel communication.

Polarization reconfigurability can also be achieved by etching cross-slots in circular patch antennas [191]. A square-ring tag antenna with circular polarization has been proposed in [192]. The AR bandwidth of the antenna is about 36 MHz (902–938 MHz), which covers the American (902–928 MHz), European (918–926 MHz), and Taiwanese (922–928 MHz) UHF RFID frequency bands. The antenna, in addition to having a simple structure, undergoes about 64% size reduction than other conventional tag antennas.

A compact, dual CP, cavity-backed ring slot antenna is proposed in [193]. The feeding network, consisting of a couple of T-– shaped capacitive feed structures, connected to a miniaturized hybrid branch line coupler makes the structure complex. The capacitive feed network also contributes to antenna matching. The measured impedance bandwidth is 12%, while the AR bandwidth is 4.8%. Due to the cavity backing, a stable gain as high as 7.4 dBi is obtained, which is quite appreciable. The designed antenna is also seen to have a significantly better FBR ratio.

In [131], the authors have presented a compact CPW-fed CP antenna. The ground plane has its corners truncated for achieving broadband response. A significantly wide impedance bandwidth of 103% and an AR bandwidth of 59% are obtained by using a U-shaped feedline, together with an inverted L-strip and a 45° tilted parasitic strip. Triangular shaped pieces cut away from the

https://doi.org/10.1017/S1759078720000331 Published online by Cambridge University Press

top corners of the antenna also contribute to the CP bandwidth. Although a wide operational bandwidth has been obtained, too many strips and structural parts make the antenna design quite complicated and also difficult to be tuned for parametric optimization.

The authors in [194] report a novel broadband dual CP microstrip-fed monopole antenna. The radiating monopole is quite novel in design, where it has been designed from an initially square monopole and then further modified by cutting bevels at the lower edges of the monopole. As a result, the monopole takes the shape of an asymmetric hexagon. The antenna is fed by two orthogonal feed lines and symmetry in the overall structure assures polarization diversity. The obtained impedance bandwidth is 149% and the AR bandwidth is 80.7%. The antenna has great usage potential in the WLAN (5, 5.2 and 5.8 GHz), WiMAX (5.5 GHz), and certain C-band communication systems operating in diverse multipath environments.

In [195], the authors have presented an advanced design approach to attain circular polarization of a microstrip antenna fed by unbalanced vertical feed lines. The design also incorporates DGS under the unbalanced feed lines to achieve circular polarization. The DGS in effect serves the purpose of tuning the impedance of the feed lines to optimize the CP bandwidth. This proposed structure avoids the design complexity of using hybrid couplers with diagonally balanced feed lines, by employing DGS. However, the obtained return loss bandwidth is 7.3%, while the AR bandwidth is only 1.9%.

In [196], the authors have presented the design of a dual-wideband printed monopole antenna for circular polarization diversity. The structure consists of a horse-shoe-shaped slot, two L-shaped radiators and is fed by two ports. The horse-shoe-shaped slot is of half wavelength resonant length. When port-I is excited and port-II is matched, the antenna radiates LHCP at the lower band and RHCP in the upper band in the positive z-direction. Upon reversing the excitation and the matched ports, the sense of CP also gets reversed. The measured return loss bandwidths are 113 and 60.2% in the lower and upper bands, respectively, while the AR bandwidths are 72.5 and 56% in the lower and upper bands, respectively. The isolation between the two excitation ports is overall better than 15 dB. The antenna response covers parts of GPS frequency range, while fully covering 2.4/5.2/5.8 GHz Bluetooth/WLAN systems and also 2.4/5.5 GHz WiFi bands.

In [197], a compact CPW-fed UWB monopole antenna with triple band CP characteristics is reported. The design introduces a rectangular stub with modified E-shaped slot to the right side of the monopole and modified I-shaped slot on the right side of the ground plane for achieving ultra-wide bandwidth of 112% (3.1–11 GHz). The proposed antenna has been fabricated on a 1-mm-thick FR4 substrate with relative permittivity of $\varepsilon_r = 4.4$ and loss tangent of $\delta = 0.02$. The overall dimension of the antenna is $(27 \times 27 \times 1)$ mm^3, while the other dimensions are $b_1 = 5$, $g1 = 7.70$, $r_1 = 6.90$, $b_2 = 4$, $g_2 = 0.25$, $r_2 = 1$, $b_3 = 0.60$, $g_3 = 8.13$, $r3 = 3.50$, $b4 = 6.90$, $g_4 = 6.50$, $r_4 = 5.10$, $b_5 = 2.65$, $g_5 = 2.85$, $r_5 = 1$, $p_1 = 1.50$, $p_6 = 0.75$, $a_5 = p2 = 0.36$, $p_7 = 2$, $a1 = 2$, $a2 = 1$, $p3 = 1.25$, $p_9 = 0.25$, $a3 = a4 = 1$, $p_4 = 0.75$, $p_{10} = 2.5$, $a_5 = a_6 = 1$, $p_5 = 1.90$, $p_8 = 1.25$, $a_7 = 1.60$.

Triple band CP characteristics are achieved by introducing modified T-shaped slot created on the left side of the ground plane along with existing I-shaped slot, fractal parasitic ring resonator, triangular step-sized ring resonator, and upper rectangular ring resonators attached with the monopole. Figure 12(b) depicts the surface current distribution of the proposed antenna at the center frequency of second CP band at 5.52 GHz. At 0° phase, the current density dominates mainly on triangular stepped ring resonator, upper rectangular ring resonator, and in addition to modified "T"- and "I"-shaped slots. The dominating currents on the surface of the modified "T"- and "I"-shaped slot are not taken into account as the horizontal and vertical currents on that surface are affected with corresponding components of each other. So, it is obvious from the analysis that the dominant current vector rotates in clockwise direction as the phase advances from 0° to 90°, as shown in Fig. 12(c) that leads to LHCP radiation in $+Z$ direction and RHCP radiation from $-Z$ direction. The novelty of this structure lies in the design of a compact printed UWB monopole antenna with combined triple band CP characteristics which are independently controllable by adjusting the antenna design parameters.

The proposed antenna achieves good CP characteristics at Citizens Broadband Radio Services in the USA (3.55–3.72 GHz), (AMC, and WLAN upper-frequency spectrum (4.81–5.61 GHz), VSAT services & Satellite Communication and Ground Surveillance RADAR (9.29–10.95 GHz), respectively. As concerned to the functionality, the proposed antenna is geometrically compact than other contemporary antenna structure existing in the literature. The antenna also has a peak gain of 4.77 dB at 9.5 GHz and maximum radiation efficiency of 93.5% in the mid-CP band ranging from 4.81 to 5.52 GHz (Table 5).

Conclusion

The article has presented a comprehensive review of different applications of CP antenna systems in modern-day wireless communications. Although the list of notable work in this field is endless, with due respect to the works of all the researchers working tirelessly in this field, the discussion is kept limited for the brevity of the review. The review shows that CP antennas are the obvious choice for antenna engineers for combating the inherent drawbacks of linearly polarized systems, like loss due to polarization mismatch, susceptibility to multipath and fading effects, Faraday rotation, inclement weather conditions, to name a few. However, most of the primitive CP antennas were narrowband. This did draw interest in research for possible means of bandwidth enhancement. Some efforts are mentioned in this article. It was also observed that an effort to increase the bandwidth often made the overall structure bulky thereby making the design unsuitable for multi-level system implants. So the research focus has now shifted to miniaturizing the antenna structure while preserving the CP radiation. Accordingly came different design approaches like using CP DRAs, incorporating fractal geometries, metamaterial loading. Some of the design approaches are discussed in this article. It has also been particularly seen that DRAs having significantly low metallization can enhance the antenna gain and radiation efficiency, while still preserving CP response. Finally, the applications of CP antennas in band-specific applications, leading to the development of dual or multi-band antennas have been reported. These antennas can operate in several narrow communication bands like WLAN, WiMAX, WiFi, C-band, X-band, GSM, LTE, ISM to name a few. It is observed that there have been profoundly many reported novel structures to achieve multiband CP characteristics. Architectural novelty is employed not only in the radiator but also in the feed network. Although such approaches can make the design bit complicated, they also increase possible design options enormously, which

https://doi.org/10.1017/S1759078720000331 Published online by Cambridge University Press

has been the motive of present-day research. Many new structures are coming up every day and updating the existing literature. The review thus finds the generation of wideband or multiband CP radiation, while simultaneously targeting overall structural compactness as the primary research motive ahead.

References

1. **Balanis CA** (2005) *Antenna Theory: Analysis and Design*, 3rd Edn. New Jersey: John Wiley & Sons, Inc.
2.. **Ludwig AC** (1975) The definition of cross-polarization. *IEEE Transactions on Antennas and Propagation* **21**, 116–119.
3. **Row JS and Ai CY** (2004) Compact design of single-feed circularly polarised microstrip antenna. *IEEE Electronics Letters* **40**, 1093–1094.
4. **James JR and Hall PS** (1989) *Handbook of Microstrip Antenna*, vol. **1**. London, UK: Peter Peregrinus Ltd.
5. **Nasimuddin N, Qing X and Chen ZN** (2009) Microstrip antenna with S-shaped slot for dual-band circularly polarized operation. *Proceedings of the European Microwave Conference*, EuMC, pp. 381–384.
6. **Li TW, Lai CL and Sun JS** (2005) Study of dual-band circularly polarized microstrip antenna. *Proceedings of the European Conference on Wireless Technology*, pp. 79–80.
7. **Haneishi M, Nambara T and Yoshida S** (1982) Study on ellipticity properties of single-feed-type circularly polarised microstrip antennas. *Electronics Letters* **18**, 191–193.
8. **Nasimuddin, Yong Y, Chen ZN and Alphones A** (2009) Circularly polarized F-shaped slot microstrip antenna with wide beamwidth. *Proceedings of the European Microwave Conference*, EuMC, pp. 1531–1534.
9. **Ravipati CB and Shafai L** (1999) A wide bandwidth circularly polarized microstrip antenna using a single feed. *Proceeding of the IEEE Antennas and Propagation Society International Symposium*, vol. 1, 244–247.
10. **Sudha T, Vedavathy TS and Bhat N** (2004) Wideband single-fed circularly polarized patch antenna. *IEEE Electronic Letters* **40**, 648–649.
11. **Iwasaki H** (1996) A circularly polarized small-size microstrip antenna with a cross slot. *IEEE Transactions on Antennas and Propagation* **44**, 1399–1401.
12. **Ali M, Dougal R, Yang G and Hwang HS** (2003) Wideband circularly polarized microstrip patch antenna for 5–6 GHz wireless LAN applications. *Proceeding of the IEEE Antennas and Propagation Society International Symposium*, vol. 2, pp. 34–37.
13. **Wang Y, Feng J, Cui J and Yang X** (2008) A dual-band circularly polarized stacked microstrip antenna with single-fed for GPS applications. *Proceedings of the 8th International Symposium on Antennas Propagation and EM Theory, ISAPE*, pp. 108–110.
14. **Chen WS, Wu CK and Wong KL** (2001) Novel compact circularly polarized square microstrip antenna. *IEEE Transactions on Antennas and Propagation* **49**, 340–342.
15. **Ullah U, Ain MF and Ahmad ZA** (2017) A review of wideband circularly polarized dielectric resonator antennas. *Communication Theories and Systems, China Communications* **14**, 65–79.
16. **Dash SKK and Khan T** (2018) Recent developments in bandwidth improvement of dielectric resonator antennas. *International Journal of RF and Microwave Computer Aided Engineering* **7**, 139518–139525.
17. **Chen WS, Wu CK and Wong KL** (1998) Compact circularly-polarised circular microstrip antenna with cross-slot and peripheral cuts. *IEEE Electronics Letters* **34**, 1040–1041.
18. **Tamakuma K and Iwasaki H** (2003) A small size circularly polarized annular microstrip antenna. *Proceedings of the International Symposium IEEE Antennas and Propagation Society*, vol. 2, pp. 716–719.
19. **Nasimuddin CZ and Qing X** (2011) Symmetric aperture antenna for broadband circular polarization. *IEEE Transactions on Antennas and Propagation* **59**, 3932–3936.
20. **Huang J** (1986) A technique for an array to generate circular polarization with linearly polarized elements. *IEEE Transactions on Antennas and Propagation* **34**, 1113–1124.
21. **Chan KKM, Tan AEC and Rambabu K** (2013) Decade bandwidth circularly polarized antenna array. *IEEE Transactions on Antennas and Propagation* **61**, 5435–5443.
22. **Yang SLS, Kishk AA and Lee KF** (2008) Wideband circularly polarized antenna with L-shaped slot. *IEEE Transactions on Antennas Propagation* **56**, 1780–1783.
23. **Tseng LY and Han TY** (2008) Microstrip-fed circular slot antenna for circular polarization. *Microwave and Optical Technology Letters* **50**, 1056–1058.
24. **Sze JY, Hsu CIG, Chen ZW and Chang CC** (2010) Broadband CPW-fed circularly polarized square slot antenna with lightening shaped feed-line and inverted-L grounded strips. *IEEE Transactions on Antennas and Propagation* **58**, 973–977.
25. **Pourahmadazar J, Ghobadi C, Nourinia J, Felegari N and Shirzad H** (2011) Broadband CPW-Fed circularly polarized square slot antenna with inverted-L strips for UWB applications. *IEEE Antennas and Wireless Propagation Letters* **10**, 369–372.
26. **Narbudowicz A, John M, Sipal V, Bao X and Amman M** (2015) Design method for wideband circularly polarized slot antennas. *IEEE Transactions on Antennas and Propagation* **63**, 4271–4279.
27. **Ellis M, Zhao Z, Wu J, Ding J, Nie Z and Liu Q** (2016) A novel simple and compact microstrip fed circularly polarized wide slot antenna with axial ratio bandwidth for C band applications. *IEEE Transactions on Antennas and Propagation* **64**, 1552–1555.
28. **Nakano H, Nogami K, Arai S, Mimaki H and Yamauchi J** (1986) A spiral antenna backed by reflector a conducting plane. *IEEE Transactions on Antennas and Propagation* **34**, 791–796.
29. **Li RL, DeJean G, Laskar J and Tentzeris MM** (2005) Investigation of circularly polarized loop antennas with a parasitic element for bandwidth enhancement. *IEEE Transactions on Antennas and Propagation* **53**, 3930–3939.
30. **Zhang Y and Zhu L** (2006) Printed dual spiral-loop wire antenna for broadband circular polarization. *IEEE Transactions on Antennas Propagation* **54**, 284–288.
31. **Hung KF and Lin YC** (2010) Novel broadband circularly polarized cavity backed aperture antenna with traveling wave excitation. *IEEE Transactions on Antennas and Propagation* **58**, 35–42.
32. **Qu SW, Chan CH and Xue Q** (2010) Wideband and high-gain composite cavity-backed crossed triangular bowtie dipoles for circularly polarized radiation. *IEEE Transactions on Antennas and Propagation* **58**, 3157–3164.
33. **Baik JW, Lee TH, Pyo S, Han SM, Jeong J and Kim YS** (2011) Broadband circularly polarized crossed dipole with parasitic loop resonators and its arrays. *IEEE Transactions on Antennas and Propagation* **59**, 80–88.
34. **He YJ, He W and Wong H** (2014) A wideband circularly polarized crossdipole antenna. *IEEE Antennas and Wireless Propagation Letters* **13**, 67–70.
35. **Chung KL** (2010) A wideband circularly polarized H-shaped patch antenna. *IEEE Transactions on Antennas and Propagation* **58**, 3379–3383.
36. **Oraizi H and Pazoki R** (2013) Wideband circularly polarized aperture-fed rotated stacked patch antenna. *IEEE Transactions on Antennas and Propagation* **61**, 1048–1054.
37. **Yang WW and Zhou JY** (2014) Wideband circularly polarized cavity-backed aperture antenna with a parasitic square path. *IEEE Antennas and Wireless Propagation Letters* **13**, 197–200.
38. **Yang W, Zhou J, Yu Z and Li L** (2014) Single-fed low profile broadband circularly polarized stacked patch antenna. *IEEE Transactions on Antennas and Propagation* **62**, 5406–5410.
39. **Guo YX, Bian L and Shi XQ** (2009) Broadband circularly polarized annular-ring microstrip antenna. *IEEE Transactions on Antennas and Propagation* **57**, 2474–2477.
40. **Mak KM and Luk KM** (2009) A circularly polarized antenna with wide axial ratio beamwidth. *IEEE Transactions on Antennas and Propagation* **57**, 3309–3312.
41. **Zhang ZY, Liu NW, Zhao JY and Fu G** (2013) Wideband circularly polarized antenna with gain improvement. *IEEE Antennas and Wireless Propagation Letters* **12**, 456–459.

https://doi.org/10.1017/S1759078720000331 Published online by Cambridge University Press

42. **Fu S, Kong Q, Fang S and Wang Z** (2014) Broadband circularly polarized microstrip antenna with coplanar parasitic ring slot patch for L-band satellite system application. *IEEE Antennas and Wireless Propagation Letters* **13**, 943–946.
43. **Ahmed OMH and Sebak AR** (2009) A novel maple-leaf shaped UWB antenna with a 5.0–6.0 GHz band-notch. *Progress in Electromagnetic Research C* **11**, 39–49.
44. **Mextorf H, Martens R, Daschner F and Knochel R** (2010) Dual polarized UWB antenna for free-space characterization of dielectric objects. *German Microwave Conference*.
45. **Zhao D, Yang C, Zhu M and Chen Z** (2016) Design of WLAN/LTE/UWB antenna with improved pattern uniformity using ground-cooperative radiating structure. *IEEE Transactions on Antennas and Propagation* **64**, 271–276.
46. **Zehforoosh Y, Ghobadi C and Nourinia J** (2006) Antenna design for ultra wideband application using a new multilayer structure. *Progress in Electromagnetics Research* **2**, 544–549.
47. **Choi J, Hong S and Kim U** (2007) The design of an UWB antenna with notch characteristics. *Progress in Electromagnetics Research* **3**, 987–990.
48. **Tang MC, Shi T and Ziolkowski W** (2016) Planar ultra wideband antennas with improved realized gain performance. *IEEE Transactions on Antennas and Propagation* **64**, 61–69.
49. **Jou CF, Wu JW and Wang CJ** (2009) Novel broadband monopole antennas with dual-band circular polarization. *IEEE Transactions on Antennas and Propagation* **57**, 1027–1034.
50. **Banerjee U, Karmakar A, Chakraborty P and Saha A** (2019) A CPW-fed compact monopole antenna with defected ground structure and modified parasitic hilbert strip having wideband circular polarization. *International Journal of Electronics and Communications (AEU)*, 110, doi: 10.1016/j.aeue.2019.152831.
51. **Pancera E** (2010) *Medical Applications of the Ultra Wideband Technology*. IEEE, Loughborough, UK.
52. **Richtmyer R** (1939) Dielectric resonators. *Journal of Applied Physics* **10**, 391–398.
53. **Long S, McAllister M and Liang S** (1983) The resonant cylindrical dielectric cavity antenna. *IEEE Transactions on Antennas and Propagation* **31**, 406–412.
54. **Agarwal S, Gupta RD, Parihar MS and Kondekar PN** (2017) A wideband high gain dielectric resonator antenna for RF energy harvesting applications. *International Journal of Electronics and Communications (AEU)* **78**, 24–31.
55. **Mongia RK and Ittipiboon A** (1997) Theoretical and experimental investigations on rectangular dielectric resonator antennas. *IEEE Transactions on Antennas and Propagation* **45**, 1348–1356.
56. **Denidni TA, Rao Q and Sebak AA** (2005) Broadband L-shaped dielectric resonator antenna. *IEEE Antennas and Wireless Propagation Letters* **4**, 453–454.
57. **Guha D and Antar YMM** (2006) New half-hemispherical dielectric resonator antenna for broadband monopole-type radiation. *IEEE Transactions on Antennas and Propagation* **54**, 3621–3628.
58. **Chair R, Kishk AA and Lee KF** (2007) Wideband stair-shaped dielectric resonator antennas. *IET Microwave Antennas Propagation* **1**, 299–305.
59. **Karmakar, DP, Soren D, Ghatak R, Poddar DR and Mishra RK** (2009) A wideband Sierpinski carpet fractal cylindrical dielectric resonator antenna for X-band application. *Proceedings of IEEE Applied Electromagnetic Conference*, pp. 1–3.
60. **Kishk AA** (2002) Tetrahedron and triangular dielectric resonator with wideband performance. *Proceedings of IEEE Antennas and Propagation Society International Symposium*, vol. 4, pp. 462–465.
61. **Kishk AA** (2003) Wide-band truncated tetrahedron dielectric resonator antenna excited by a coaxial probe. *IEEE Transactions on Antennas and Propagation* **51**, 2913–2917.
62. **Kishk AA, Glisson AW and Junker GP** (2001) Bandwidth enhancement for a split cylindrical dielectric resonator antenna. *Progress in Electromagnetics Research*, **33**, 97–118.
63. **Coulibaly Y, Denidni TA and Boutayeb H** (2008) Broadband microstrip-fed dielectric resonator antenna for X-band applications. *IEEE Antennas and Wireless Propagation Letters* **7**, 341–345.
64. **Chang TH and Kiang JF** (2007) Broadband dielectric resonator antenna with metal coating. *IEEE Transactions on Antennas and Propagation*, **55**, 1254–1259.
65. **Denidni TA and Weng Z** (2011) Hybrid ultra wideband dielectric resonator antenna and band notched designs. *IET Microwave Antennas and Propagation* **5**, 450–458.
66. **Lin YF, Chen HM and Lin CH** (2009) Compact dual-band hybrid dielectric resonator antenna with radiating slot. *IEEE Antennas and Wireless Propagation Letters* **8**, 6–9.
67. **Gao Y, Feng Z and Zhang L** (2011) Compact CPW-fed dielectric resonator antenna with dual polarization. *IEEE Antennas and Wireless Propagation Letters* **10**, 544–547.
68. **Chair R, Kishk AA, Lee KF and Smith CE** (2004) Wideband flipped staired pyramid dielectric resonator antennas. *Electronic Letters* **40**, 581–582.
69. **Chang TH and Kiang JF** (2007) Broadband dielectric resonator antenna with an offset well. *IEEE Antennas and Wireless Propagation Letters* **6**, 564–567.
70. **Leung KW and So KK** (2009) Theory and experiment of the wideband two-layer hemispherical dielectric resonator antenna. *IEEE Transactions on Antennas and Propagation* **57**, 1280–1284.
71. **Eshrah IA, Kishk AA, Yakovlev AB and Glisson AW** (2005) Excitation of dielectric resonator antennas by a waveguide probe, modeling technique and wideband design. *IEEE Transactions on Antennas and Propagation* **53**, 1028–1037.
72. **Leung KW and So KK** (2001) Waveguide excited dielectric resonator antenna. *Proceedings of the IEEE Antennas and Propagation Society International Symposium*, pp. 132–135.
73. **Lin YF, Chen HM, Lin CY and Pan SC** (2009) Planar inverted L-antenna with a dielectric resonator feed in a mobile device. *IEEE Transactions on Antennas and Propagation* **57**, 3342–3346.
74. **Hadi LK, Kishk AA and Kajfez D** (2009) Triple mode use of a single dielectric resonator. *IEEE Transactions on Antennas and Propagation* **57**, 1328–1335.
75. **Huitema L, Koubeissi M, Mouhamadou M, Arnaud E, Decroze E and Monediere T** (2011) Compact and multi-band dielectric resonator antenna with pattern diversity for multistandard mobile handheld devices. *IEEE Transactions on Antennas and Propagation* **59**, 4201–4208.
76. **Kishk AA, Ahn B and Kajfez D** (1989) Broadband stacked dielectric resonator antennas. *Electronic Letters* **25**, 1232–1233.
77. **Rao Q, Denidni TA and Sebak AR** (2006) Broadband compact stacked T-shaped DRA with equilateral triangle cross-sections. *IEEE Microwave and Wireless Communication Letters* **16**, 7–9.
78. **Luk KM, Lee MT, Leung KW and Yung EKN** (1999) Technique for improving coupling between microstrip line and dielectric resonator antenna. *Electronic Letters* **35**, 357–358.
79. **Li B and Leung KW** (2005) Strip fed rectangular dielectric resonator antennas with/without parasitic patch. *IEEE Transactions on Antennas and Propagation* **53**, 469–474.
80. **Leung KW and Leung CK** (2003) Wideband dielectric resonator antenna excited by cavity-backed circular aperture with microstrip tuning fork. *Electronic Letters* **39**, 1033–1035.
81. **Kishk AA, Chair R and Lee KF** (2006) Broadband dielectric resonator antenna excited by L-shaped probe. *IEEE Transactions on Antennas and Propagation* **54**, 2182–2189.
82. **Kishk AA, Chair R and Lee KF** (2006) Hook and 3D J-shaped probe excited dielectric resonator antenna for dual polarization application. *IEE Proceedings of Microwave, Antennas and Propagation*, **153**, 277–281.
83. **Kishk AA, Lee KF and Chair R** (2005) Wideband simple cylindrical dielectric resonator antennas. *IEEE Microwave and Wireless Communication Letters* **15**, 241–243.
84. **De Young CS and Long SA** (2006) Wideband cylindrical and rectangular dielectric resonator antennas. *IEEE Antennas and Wireless Propagation Letters* **5**, 426–429.
85. **Fan Z and Antar YMM** (1997) Slot-coupled dielectric resonator antenna for dual frequency operation. *IEEE Transactions on Antennas and Propagation* **45**, 306–308.

https://doi.org/10.1017/S1759078720000331 Published online by Cambridge University Press

86. **Nannini C, Ribero M, Dauvignac JY and Pichot C** (2003) A dual frequency dielectric resonator antenna. *Microwave and Optical Technology Letters* **38**, 9–10.
87. **Lin YF, Lin CH, Chen HL and Hall PS** (2006) A miniature dielectric loaded monopole antenna for 2.4/5 GHz WLAN applications. *IEEE Microwave and Wireless Communication Letters* **16**, 591–593.
88. **Guha D and Antar YMM** (2006) Four element cylindrical dielectric resonator antenna for wideband monopole like radiation. *IEEE Transactions on Antennas and Propagation* **52**, 2657–2662.
89. **Haneishi M and Takazawa H** (1985) Broadband circularly polarized planar array composed of a pair of dielectric resonator antennas. *Electronic Letters* **21**, 437–438.
90. **Mongia RK, Ittipiboon A, Cuhaci M and Roscoe D** (1994) Circularly polarized dielectric resonator antenna. *Electronic Letters* **30**, 1361–1362.
91. **Esselle KP** (1996) Circularly polarized higher order rectangular dielectric resonator antenna. *Electronic Letters* **32**, 150–151.
92. **Leung KW, Wong WC, Luk KM and Yung EKN** (2000) Circularly polarized dielectric resonator antenna excited by dual conformal strips. *Electronic Letters* **36**, 484–486.
93. **Leung KW and Mok SK** (2001) Circularly polarized dielectric resonator antenna excited by perturbed annular slot with backing cavity. *Electronic Letters* **37**, 934–936.
94. **Chair R, Kishk AA, Yang SLS, Lee KF and Luk KM** (2006) Aperture fed wideband circularly polarized rectangular stair-shaped dielectric resonator antenna. *IEEE Transactions on Antennas and Propagation* **54**, 1350–1352.
95. **Guha D, Antar YMM and Chu LCY** (2006) Comb-shaped circularly polarized dielectric resonator antenna. *Electronic Letters* **42**, 785–787.
96. **Mongia RK** (1989) Half-split dielectric resonator placed on a metallic plane for antenna applications. *Electronic Letters* **25**, 463–464.
97. **Tam MTK and Murch RD** (1999) Compact circular sector and annular sector dielectric resonator antenna. *IEEE Transactions on Antennas and Propagation* **47**, 837–842.
98. **Hady LK, Kishk AA and Kajfez D** (2009) Dual – band compact DRA with circular and monopole – like linear polarizations as a concept for GPS and WLAN applications. *IEEE Transactions on Antennas and Propagation* **57**, 2591–2598.
99. **Li B, Hao CX and Sheng XQ** (2009) A dual-mode quadrature-fed wideband circularly polarized dielectric resonator antenna. *IEEEAntennas and Wireless Propagation Letters* **8**, 1036–1038.
100. **Chan R, Zhong SS and Liu J** (2014) Broadband circularly polarized dielectric resonator antenna fed by wideband switched line coupler. *Electronic Letters* **50**, 725–726.
101. **Petosa A, Ittipiboon A and Cuhaci M** (1996) Array of circularly polarized cross dielectric resonator antennas. *Electronic Letters* **32**, 1742–1743.
102. **Laisne A, Gillard R and Piton G** (2002) Circularly polarized dielectric resonator antenna with metallic strip. *Electronic Letters* **38**, 106–107.
103. **Yang SI, Chair R and Kishk AA** (2007) Study on sequential feeding networks for Sub-arrays of circularly polarized elliptical dielectric resonator antennas. *IEEE Transactions on Antennas and Propagation* **55**, 321–333.
104. **Fakhte S, Oraizi H and Karimian R** (2014) A novel low-cost circularly polarized rotated stacked dielectric resonator antenna. *IEEE Antennas and Wireless Propagation Letters* **13**, 722–725.
105. **Mandelbrot B** (1982) *The Fractal Geometry of Nature*. San Francisco: W. H. Freeman and Co., pp. 1186–1189.
106. **Werner DH and Ganguly S** (2003) An overview of fractal antenna engineering research. *IEEE Antennas and Propagation Magazine* **45**, 38–57.
107. **Anguera J, Puente C, Borja C and Soler J** (2005) Fractal shaped antennas: a review. *Encyclopedia of RF and Microwave Engineering* **2**, 1620–1635.
108. **Martinez E, Anguera J, Puente C, Borja C and Soler J** (2004) Broadband dual-frequency microstrip patch antenna with modified sierpinski fractal geometry. *IEEE Transactions on Antennas and Propagation* **52**, 66–73.
109. **Pakkathillam JK, Kanagasabai M, Varadhan C and Sakthivel P** (2013) A novel fractal antenna for UHF near-field RFID reader. *IEEE Antennas and Wireless Propagation Letters* **12**, 1141–1144.
110. **Farswan A, Gautam AK, Kanaujia BK and Rambabu K** (2016) Design of koch fractal circularly polarized antenna for handheld UHF RFID reader applications. *IEEE Transactions on Antennas and Propagation* **64**, 771–775.
111. **Wei K, Li J, Wang L, Xu R and Xing Z** (2017) A New technique to design circularly polarized microstrip antenna by fractal defected ground structure. *IEEE Transactions on Antennas and Propagation* **65**, 3721–3725.
112. **Pakkathillam JK and Kanagasabai M** (2015) Circularly polarized broadband antenna deploying fractal slot geometry. *IEEE Antennas and Wireless Propagation Letters* **14**, 1286–1289.
113. **Jayakrighnan VM and Sreedevi KM** (2017) Circular microstrip patch assisted planar cross-over for GPS application. *Progress in Electromagnetics Research Symposium – Spring* (*PIERS*), St. Petersburg. Russia.
114. **Joy S, Natarajamani S and Vaitheeswaran SM** (2018) Minkowski fractal circularly polarized planar antenna for GPS application. *Proceedings of the8th International Conference on Advances in Computing and Communication (ICACC)*, vol. 143, pp. 66–73.
115. **Biswas S, Guha D and Kumar C** (2013) Control of higher harmonics and their radiation in microstrip antennas using compact defected ground structures. *IEEE Transactions on Antennas and Propagation* **61**, 3349–3354.
116. **Zulkifli FY, Rahardjo ET and Hartanto D** (2008) Radiation properties enhancement of triangular patch microstrip antenna array using hexagonal defected ground structure. *Progressin Electromagnetics Research* **5**, 101–109.
117. **Chi PL, Waterhouse R and Itoh T** (2011) Antenna miniaturization using slow wave enhancement factor from loaded transmission line models. *IEEE Transactions on Antennas and Propagation* **59**, 48–57.
118. **Kim HM and Lee B** (2006) Bandgap and slow/fast wave characteristics of defected ground structures including left-handed features. *IEEE Transactions on Microwave Theory and Technology* **54**, 3113–3120.
119. **Prajapati PR, Krishnamurthy GG, Patnaik A and Kartikeyan MV** (2015) Design and testing of a compact circularly polarized microstrip antenna with fractal defected ground structure for L-band applications. *IET Microwaves. Antennas and Propagation* **9**, 1179–1185.
120. **Reddy VV and Sarma NVSN** (2014) Single feed circularly polarized poly fractal antenna for wireless applications. *International Journal of Computer and Information Technology* **8**, 1710–1713.
121. **Reddy VV and Sarma NVSN** (2014) Triband circularly polarized Koch fractal boundary microstrip antenna. *IEEE Antennas and Wireless Propagation Letters* **13**, 1057–1060.
122. **Baliarda CP, Romeu J and Cardama A** (2000) The Koch monopole: a small fractal antenna. *IEEE Transactions on Antennas and Propagation* **48**, 1773–1781.
123. **Rao PN and Sarma NVSN** (2008) Fractal boundary circularly polarized single feed microstrip antenna. *Electronic Letters* **44**, 1710–1711.
124. **Arezoomand AS, Zarrabi FB, Heydari S and Gandji NP** (2015) Independent polarization and multi-band THz absorber base on Jerusalem cross. *Optics Communications* **352**, 121–126.
125. **Wang GD, Liu MH, Hu XW, Kong LH, Cheng LL and Chen ZQ** (2014) Multi-band microwave metamaterial absorber based on coplanar Jerusalem crosses. *Chinese Physics B* **23**, 017802.
126. **Zarrabi FB, Mansouri Z, Ahmadian R, Rahimi M and Kuhestani H** (2015) Microstrip slot antenna applications with SRR for WiMAX/WLAN with linear and circular polarization. *Microwave and Optical Technology Letters* **57**, 1332–1338.
127. **Row JS and Lin YD** (2014) Miniaturized designs of circularly polarized slot antenna. *Microwave and Optical Technology Letters* **56**, 1522–1526.
128. **Qing X and Chen ZN** (2014) Dual-square-ring-shaped slot antenna for wideband circularly polarized radiation. *Microwave and Optical Technology Letters* **56**, 2645–2649.
129. **Wang XY and Yang GM** (2014) Dual frequency and dual circular polarization slot antenna for BeiDou navigation satellite system applications. *Microwave and Optical Technology Letters* **56**, 2222–2225.
130. **Wei CY, Liu JC, Bor SS, Hung TF and Chen CC** (2013) Compact single-feed circular slot antenna with asymmetrical C-shaped strips for

https://doi.org/10.1017/S1759078720000331 Published online by Cambridge University Press

WLAN/WiMAX triband and circular/elliptical polarizations. *Microwave and Optical Technology Letters* **55**, 272–278.
131. **Pouyanfar N** (2013) Broadband square slot circularly polarized antenna for WiMAX and WLAN applications. *Microwave and Optical Technology Letters* **55**, 2191–2195.
132. **Heydari S, Jahangiri P, Arezoomand AS and Zarrabi FB** (2016) Circular polarization fractal slot by Jerusalem cross slot for wireless applications. *Progress in Electromagnetics Research Letters* **63**, 79–84.
133. **Oraizi H and Hedayati S** (2012) Circularly polarized multiband microstrip antenna using the square and giuseppe peano fractals. *IEEE Transactions on Antennas and Propagation* **60**, 3466–3470.
134. **Jahromi MN and Komjani N** (2008) Novel fractal monopole wideband antenna. *Electromagnetic Waves and Applications* **22**, 195–205.
135. **Blanco D, Rajo-Iglesias E, Maci S and Llombart N** (2015) Directivity enhancement and spurious radiation suppression in leaky-wave antennas using inductive grid metasurfaces. *IEEE Transactions on Antennas and Propagation* **63**, 891–900.
136. **Xu HX, Wang GM, Liang JG, Qi MQ and Gao X** (2013) Compact circularly polarized antennas combining meta-surfaces and strong spacefilling meta-resonators. *IEEE Transactions on Antennas and Propagation* **61**, 3442–3450.
137. **Martin SH, Martinez I, Turpin JP, Werner DH, Lier E and Bray MG** (2014) The synthesis of wide- and multi-bandgap electromagnetic surfaces with finite size and nonuniform capacitive loading. *IEEE Transactions on Microwave Theory and Techniques* **62**, 1962–1972.
138. **Sarrazin F, Pflaum S and Delaveaud C** (2016) Radiation efficiency optimization of electrically small antennas. *International Workshop on Antenna Technology* (*IWAT*), *USA*. doi: 10.1109/IWAT.2016.7434792.
139. **Ziolkowski RW and Erentok A** (2006) Metamaterial based efficient electrically small antennas. *IEEE Transactions on Antennas and Propagation* **54**, 2113–2130.
140. **Ziolkowski RW and Jin P** (2010) Broadband efficient electrically small metamaterial inspired antennas facilitated by active near-field resonant parasitic modes. *IEEE Transactions on Antennas and Propagation* **58**, 318–327.
141. **Park BC and Lee JH** (2011) Omnidirectional circularly polarized antenna utilizing zeroth-order resonance of epsilon negative transmission line. *IEEE Transactions on Antennas and Propagation* **59**, 2717–2721.
142. **Zhou C, Wang G, Wang Y, Zong B and Ma J** (2013) CPW-fed dualband linearly and circularly polarized antenna employing novel composite right/left-handed transmission line. *IEEE Antennas andWireless Propagation Letters* **12**, 1073–1076.
143. **Ko ST, Park BC and Lee JH** (2013) Dual band circularly polarized patch antenna with first positive and negative modes. *IEEEAntennas and Wireless Propagation Letters* **12**, 1165–1168.
144. **Cai T, Wang GM, Zhang XF and Shi JP** (2015) Low-profile compact circularly-polarized antenna based on fractal metasurface and fractal resonator. *IEEE Antennas and Wireless Propagation Letters* **14**, 1072–1076.
145. **Han W, Yang F, Long R, Zhou L and Yan F** (2015) Bandwidth enhancement for single-feed circularly polarized microstrip antenna with epsilon-negative transmission line-based annular ring. *Electronic Letters* **51**, 1475–1476.
146. **Chu QX, Ye M and Li XR** (2017) A low-profile omnidirectional circularly polarized antenna using planar sector-shaped endfire elements. *IEEE Transactions on Antennas and Propagation* **65**, 2240–2247.
147. **Caloz C and Itoh T** (2005) *Electromagnetic Metamaterials: Transmission Line Approach and Microwave Applications*. New York: Wiley.
148. **Sharma SK and Chaudhary RK** (2015) A compact zeroth-order resonating wideband antenna with dual-band characteristics. *IEEE Antennas and Wireless Propagation Letters* **14**, 1670–1672.
149. **Ameen M and Chaudhary RK** (2018) Metamaterial based circularly polarized antenna employing ENG-TL with enhanced bandwidth for WLAN applications. *Electronic Letters* **54**, 1152–1154.
150. **Yu A, Yang F and Elsherbeni A** (2008) A dual band circularly polarized ring antenna based on composite right and left handed metamaterials. *Progress in Electromagnetics Research* **78**, 73–81.
151. **Smith DR, Pendry JB and Wiltshire MCK** (2004) Metamaterials and negative refractive index. *Science (New York, N.Y.)* **305**, 788.
152. **Jackson JD** (1999) *Classical Electrodynamics*, 3rd Edn. New York: Wiley.
153. **Cheng YZ, Nie Y, Cheng ZZ, Wang X and Gong RZ** (2013) Asymmetric chiral metamaterial circular polarizer based on twisted split ring resonator. *Applied Physics B, Lasers and Optics*, 116. doi: 10.1007/s00340-013-5659-z.
154. **Prakash P, Abegaonkar MP, Basu A and Koul SK** (2013) Gain enhancement of a CPW-fed monopole antenna using polarization insensitive AMC structure. *IEEE Antennas and Wireless Propagation Letters* **12**, 1315–1318.
155. **Jiang ZH, Brocker DE, Sieber PE and Werner DH** (2013) A compact, low-profile metasurface-enabled antenna for wearable medical body area network devices. *IEEE Transactions on Antennas and Propagation* **62**, 4021–4030.
156. **Wu Q, Scarborough CP, Werner DH, Lier E and Wang X** (2012) Design synthesis of metasurfaces for broadband hybrid-mode horn antennas with enhanced radiation pattern and polarization characteristics. *IEEE Transactions on Antennas and Propagation* **60**, 3594–3604.
157. **Liu W, Chen ZN and Qing X** (2014) Metamaterial-based low-profile broadband mushroom antenna. *IEEE Transactions on Antennas and Propagation* **62**, 1165–1172.
158. **Yang F, Demir V, Elsherbeni DA, Elsherbeni AZ and Eldek AA** (2005) Planar dipole antennas near the edge of an EBG ground plane. *Proceedings on Antennas and Propagation Symposium*, vol. 1A, pp. 750–753.
159. **Cao WQ, Zhang BN, Liu AJ, Yu TB, Guo DS and Pan XF** (2012) Multi-frequency and dual-mode patch antenna based on electromagnetic band-gap (EBG) structure. *IEEE Transactions on Antennas and Propagation* **60**, 6007–6012.
160. **Ding K, Gao C, Liu AJ, Yu T and Qu D** (2015) Broadband C-shaped circularly polarized monopole antenna. *IEEE Transactions on Antennas and Propagation* **63**, 785–790.
161. **Li GH, Zhai HQ TL and Liang CH** (2012) A compact antenna with broad bandwidth and quad- sense circular polarization. *IEEE Transactions on Antennas and Wireless Propagation* **11**, 761–794.
162. **Rui X, Li J and Wei K** (2016) Dual-band dual-sense circularly polarized square slot antenna with simple structure. *Electronic Letters* **52**, 578–580.
163. **Guo D, He K, Zhang Y and Song M** (2017) A multibanddual-polarized omni-directional antenna for indoor wireless communication systems. *IEEE Antennas and Wireless Propagation Letters* **16**, 290–293.
164. **Tran HH and Park I** (2016) A dual-wideband circularly polarized antenna using an artificial magnetic conductor. *IEEE Antennas and Wireless Propagation Letters* **15**, 950–953.
165. **Yang W, Che W, Jin H, Feng W and Xue Q** (2015) A polarization-reconfigurable dipole antenna using polarization rotation AMC structure. *IEEE Transactions on Antennas and Propagation* **63**, 5305–5315.
166. **Huang C, Pan W, Ma X and Luo X** (2015) Wideband radar cross-section reduction of a stacked patch array antenna using metasurface. *IEEE Antennas and Wireless Propagation Letters* **14**, 1369–1372.
167. **Xiong X, Li X, Zhang W and Zhang H** (2018) Enhance dual-band circularly polarized broadband antenna by using parasitic patch. *IET Microwaves, Antennas and Propagation* **12**, 2085–2088.
168. **Paracha KN, Abdul Rahim SK, Soh PJ, Kamarudin MR, Tan KG, Lo YC and Islam MT** (2019) A Low profile, dual-band, dual polarized antenna for indoor/outdoor wearable application. *IEEE Access* **7**, 33277–33288.
169. **Ghaffarian MS, Moradi G and Mousavi P** (2017) Wide band circularly polarized slot antenna by using artificial transmission line. *IET Microwaves, Antennas & Propagation* **11**, 672–679.
170. **Torres-Garcia A, Marante F, Tazon A, Vassal'lo J, Teniente J and Beruete M** (2016) Broadband circular polarized field generation in single layer microstrip patch antennas. *Proceedings of the10th European Conference on Antennas and Propagation (Eucap)*.
171. **Torres AE, Marante F, Tazón A and Vassal'lo J** (2015) New microstrip radiator feeding by electromagnetic coupling for circular polarization. *International Journal of Electronics and Communications (AEU)* **69**, 1880–1884.
172. **Mohamed HA and Sultan KS** (2018) Quad band monopole antenna for Iot applications. *Proceedings of the IEEE International Symposium on*

https://doi.org/10.1017/S1759078720000331 Published online by Cambridge University Press

Antennas and Propagation & USNC/URSI National Radio Science Meeting.
173. **Hsu CW, Shih MH and Wang CJ** (2016) A triple-strip monopole antenna with dual-band circular polarization. *Proceedings of the IEEE 5th Asia-Pacific Conference on Antennas and Propagation (APCAP)*, pp. 137–138.
174. **Tan MT and Wang BZ** (2016) A dual-band circularly polarized planar monopole antenna for WLAN/Wi-Fi applications. *IEEE Antennas and Wireless Propagation Letters* **15**, 670–673.
175. **Chen CH and Yung EKN** (2011) Dual-band circularly-polarized CPW-fed slot antenna with a small frequency ratio and wide bandwidths. *IEEE Transactions on Antennas and Propagation* **59**, 1379–1384.
176. **Chen HD and Chen HT** (2004) A CPW-fed dual-frequency monopole antenna. *IEEE Transactions on Antennas and Propagation* **52**, 978–982.
177. **Abed AT, Singh MJ and Islam MT** (2018) Compact fractal antenna circularly polarized radiation for Wi-Fi and WiMAX communications. *IET Microwaves Antennas and Propagation* **12**, 2218–2224.
178. **Altaf A and Seo M** (2018) A tilted D-shaped monopole antenna with wide dual-band dual-sense circular polarization. *IEEE Antennas and Wireless Propagation Letters* **12**, 2464–2468.
179. **Liang W, Jiao YC, Luan Y and Tian C** (2015) A dual-band circularly polarized complementary antenna. *IEEE Antennas and Wireless Propagation Letters* **14**, 1153–1156.
180. **Xu R, Li J, Qi YX, Guangwei Y and Yang JJ** (2017) A design of triple-wideband triple-sense circularly polarized square slot antenna. *IEEE Antennas and Wireless Propagation Letters* **16**, 1763–1766.
181. **Qin PY, Guo YJ and Liang CH** (2010) Effect of antenna polarization diversity on MIMO system capacity. *IEEE Antennas and Wireless Propagation Letters* **9**, 1092–1095.
182. **Khidre A, Lee KF, Yang Y and Elsherbeni AZ** (2013) Circular polarization reconfigurable wideband E-shaped patch antenna for wireless applications. *IEEE Transactions on Antennas and Propagation* **61**, 960–964.
183. **Khaleghi A and Kamyab M** (2009) Reconfigurable single port antenna with circular polarization diversity. *IEEE Transactions on Antennas and Propagation* **57**, 555–559.
184. **Saini RK and Dwari S** (2016) Broadband dual circularly polarized square slot antenna. *IEEE Transactions on Antennas and Propagation* **64**, 290–294.
185. **Chen YB, Jiao YC and Zhang FS** (2007) Polarization reconfigurable CPW-fed square slot antenna using PIN diodes. *Microwave and Optical Technology Letters* **49**, 1233–1236.
186. **Kumar P, Dwari S, Saini RK and Mandal MK** (2019) Dual-band dual-sense polarization reconfigurable circularly polarized antenna. *IEEE Antennas and Wireless Propagation Letters* **18**, 64–68.
187. **Zhang XY, Zhang Y, Pan YM and Duan W** (2017) Low-profile dual-band filtering patch antenna and its application to LTE MIMO system. *IEEE Transactions on Antennas and Propagation* **65**, 103–113.
188. **Li JF, Wu DL, Zhang G, Wu YJ and Mao CX** (2019) A left/right-handed dual circularly-polarized antenna With duplexing and filtering performance. *IEEE Access* **7**, 35431–35437.
189. **Wang L, Guo YX and Sheng W** (2012) Tri-Band circularly polarized annular slot antenna for GPS and CNSS applications. *IEEE Antennas and Wireless Propagation Letters (Early Access)*, 26. doi: 10.1109/LAWP.2012.2200869.
190. **Liang Z, Li Y and Long Y** (2014) Multiband monopole Mobile phone antenna with circular polarization for GNSS application. *IEEE Transactions on Antennas and Propagation* **62**, 1910–1917.
191. **Osman MN, Rahim MKA, Yussof MFM, Hamid MR and Majid HA** (2013) Polarization reconfigurable cross-slots circular patch antenna. *Proceedings of the International Symposium of Antennas and Propagation*, vol. 2, pp. 1252–1255.
192. **Lu JH and Chang BS** (2017) Planar compact square-ring tag antenna with circular polarization for UHF RFID applications. *IEEE Transactions on Antennas and Propagation* **65**, 432–441.
193. **Ferreira R, Joubert J and Odendaal JW** (2017) A compact dual-circularly polarized cavity-backed ring-slot antenna. *IEEE Transactions on Antennas and Propagation* **65**, 364–368.
194. **Chandu DS and Karthikeyan SS** (2017) A novel broadband dual circularly polarized microstrip-fed monopole antenna. *IEEE Transactions on Antennas and Propagation* **65**, 1410–1415.
195. **Thakur JP and Park JS** (2006) An advance design approach for circular polarization of the microstrip antenna with unbalance DGS feedlines. *IEEE Antennas and Wireless Propagation Letters* **5**, 101–103.
196. **Xu R, Li JY, Liu J, Zhou SG, Xing ZJ and Wei K** (2018) A design of dual-wideband planar printed antenna for circular polarization diversity by combining slot and monopole modes. *IEEE Transactions on Antennas and Propagation* **66**, 4326–4331.
197. **Karmakar A, Banerjee U, Chakraborty P and Saha A** (2019) Combined triple-band circularly polarized and compact UWB monopole antenna. *IET Microwaves Antennas and Propagation* **13**, 1306–1311.



Mr. Utsab Banerjee belongs from Kolkata, West Bengal, India. He received his B.Tech degree in Electronics and Communication Engineering and M.Tech degree in Communication Engineering, both from Netaji Subhash Engineering College, under West Bengal University of Technology, Kolkata, West Bengal, India in 2010 and 2013, respectively. He is currently a Research Scholar in the Department of Electronics and Communication Engineering, Tripura University (A Central University), Suryamaninagar, Tripura, India. His research interests include analysis and design of compact antennas for wideband applications, ultra-wideband antennas, fractal antennas, various Circularly Polarized antennas, such as wide band, multiband, as well as antennas having special applications such as GPS, RFID etc, circularly polarized dielectric resonator antennas. He is also active in the study of electromagnetic wave theory and the antenna theory. He has published a number of peer-reviewed journal papers and conference articles. He has been awarded with the "Research Excellence Award" by the Institute of Scholars (INSc).



Dr. Anirban Karmakar has completed his Ph.D. in Engineering from Jadavpur University, Kolkata, India, in 2015. He has more than 13 years of teaching experience and is currently holding the post of Assistant Professor in the Department of Electronics & Communication Engineering at Tripura University, A Central University, India. He has almost 40 research articles in refereed journals and international conference proceedings. He has served as a reviewer in different international journals. He was awarded the best paper award from different international conferences. He is a Senior Member of IEEE and has organized different workshops in the capacity of a convener and completed various funded projects received from UGC. His areas of interest include planar and fractal wideband antennas, Arrays, Circular Polarized Antennas, DRA etc.



Dr. Anuradha Saha received the M.Tech. degree in Mechatronics from the National Institute of Technical Teachers' Training and Research, Kolkata in 2009 and Ph.D. degree in Engineering from Jadavpur University in 2017. She has been working as an assistant professor in the Department of Applied Electronics and Instrumentation Engineering since 2008, wherein between she has served as full-time research scholar from 2012 to 2015 at the Department of Electronics and Telecommunication Engineering of Jadavpur University, funded by UGC. She is the author of over 30 publications in top international journals and conference proceedings. Her research interests include Artificial Intelligence, Pattern Recognition, Cognitive Robotics, and Human-Computer-Interaction. She is the reviewer of some renowned journals including IEEE Transactions on Fuzzy Systems, IEEE Transactions on Emerging Topics in Computational Intelligence, IETE Journal of Research, and so on.

https://doi.org/10.1017/S1759078720000331 Published online by Cambridge University Press